Molecular Crystals and Liquid Crystals Science and Technology. Section A. Molecular Crystals and Liquid Crystals

Publication details, including instructions for authors and subscription information:
http://www.tandfonline.com/loi/gmcl19

Peculiarity Of Ethylenedioxy Group In Formation Of Conductive Charge-Transfer Complexes Of Bis(Ethylenedioxy) - Dibenzotetrathiafulvalene (BEDC-DBTTF)

T. Senga [a] , K. Kamoshida [a] , L. A. Kushch [a c] , G. Saito [a] , T. Inayoshi [b] & I. Ono [b]

[a] Division of Chemistry, Graduate School of Science, Kyoto University, Sakyo-ku, Kyoto, 606-01, Japan

[b] Department of Chemistry, College of Science and Engineering, Aoyama Gakuin University, Chitosedai, Setagaya-ku, Tokyo, 157, Japan

[c] Institute of Chemical Physics, Russian Academy of Science, Chernogolovka, Moscow District, 142432, Russia

Version of record first published: 24 Sep 2006

To cite this article: T. Senga, K. Kamoshida, L. A. Kushch, G. Saito, T. Inayoshi & I. Ono (1997): Peculiarity Of Ethylenedioxy Group In Formation Of Conductive Charge-Transfer Complexes Of Bis(Ethylenedioxy) - Dibenzotetrathiafulvalene (BEDC-DBTTF), Molecular Crystals and Liquid Crystals Science and Technology. Section A. Molecular Crystals and Liquid Crystals, 296:1, 97-143

To link to this article: http://dx.doi.org/10.1080/10587259708032316

Mol. Cryst. Liq. Cryst., 1997, Vol. 296, pp. 97–143
Reprints available directly from the publisher
Photocopying permitted by license only

PECULIARITY OF ETHYLENEDIOXY GROUP IN FORMATION OF CONDUCTIVE CHARGE-TRANSFER COMPLEXES OF BIS(ETHYLENE-DIOXY)-DIBENZOTETRATHIAFULVALENE (BEDO-DBTTF)

TAKESHI SENGA, KENTA KAMOSHIDA, LYUDMILA A. KUSHCH,[#]
GUNZI SAITO,*
Division of Chemistry, Graduate School of Science, Kyoto University, Sakyo-ku, Kyoto 606-01, Japan

TOMOKO INAYOSHI,* ISAO ONO
Department of Chemistry, College of Science and Engineering, Aoyama Gakuin University, Chitosedai, Setagaya-ku, Tokyo 157, Japan

(Received 10 October 1996; In final form 10 November 1996)

ABSTRACT The electronic and molecular structures and charge transfer (CT) complex formation of a new electron donor molecule; bis(ethylenedioxy)-dibenzotetrathiafulvalene (BEDO-DBTTF), were studied from the point of the peculiar ability of ethylenedioxy group in delivering conductive solid complexes. The BEDO-DBTTF molecules afforded 37 solid complexes with 40 kinds of electron acceptor molecules belonging to 5 systems; TCNQ, quinone, fluorene, percyano and nitrophenyl systems. The infrared and ultraviolet-visible-near infrared spectra of the complexes were examined to study the ionicity of their ground states in solid. A plot of CT transition energies and the difference of redox potentials; $\Delta E(DA)$, of donor and acceptor molecules indicated that 10 complexes have neutral ground state. No definitely identified back CT bands were observed in the 4 complexes of completely ionic ground state. 23 complexes of partially ionic ground state gave CT transitions below 5×10^3 cm^{-1} and are highly conductive. The presence of the ethylenedioxy group in BEDO-DBTTF provided wide variety of conductive complexes regardless the size and shape of acceptor molecules, with smaller degree of CT ($\gamma \geq 0.3$), from combination with much weaker acceptor molecules ($\Delta E(DA) \leq 0.53$) than expected for conventional TTF·TCNQ system ($\gamma \geq 0.5$, $\Delta E(DA) \leq 0.34$) and with donor molecule excess in content. These features are very much resemblance to those of BEDO-TTF which affords a number of metallic complexes and are ascribed to peculiar ability of ethylenedioxy group to assemble self-aggregated donor assemblies. In spite of such similarity, the partially ionic complexes of BEDO-DBTTF are not metallic, maybe due to the lack of the side-by-side intermolecular sulfur··sulfur short contacts that is predicted based on the molecular geometry consideration. Single crystal growth of BEDO-DBTTF complexes was not much successful. 2,5-Dimethyl- and 2,5-dimethoxy-TCNQ complexes, which reside near the boundary of the partial CT and neutral states, afforded complexes with different ionicities, conductivities and optical properties. The crystal structures of neutral complexes of 2,5-dimethyl- and 2,5-dimethoxy-TCNQ as well as that of neutral donor molecules were determined.

Keywords: ethylenedioxy group, BEDO-DBTTF, molecular conductor, charge-transfer complex, ionicity

---

Permanent address: Institute of Chemical Physics, Russian Academy of Science, Chernogolovka, Moscow District 142432, Russia.

INTRODUCTION

The bis(ethylenedioxy)-tetrathiafulvalene (BEDO-TTF (BO), Scheme 1, for abbreviation of all chemicals in text, see ref. 1) molecule is known to exert strong ability to form conductive charge-transfer (CT) complexes with a large variety of organic acceptors and organic or inorganic anions.[2] Although size and strength of the organic acceptors vary widely, metallic conductivity is observed in most cases. In particular, this donor provides a number of organic metals with smaller degree of CT and from the combination with much weaker acceptors than expected for the conventional TTF·TCNQ type low-dimensional organic metals. Furthermore, this donor provides CT complexes of excess content of the donor molecule, which allows the partial CT ground state in the complexes with strong acceptor molecules. On the other hand, its sulfur analog; BEDT-TTF (ET), affords not so many metallic CT complexes with organic acceptors and the stoichiometries of them are mainly 1:1,[3] though it gives a number of two-dimensional (2D) metals and superconductors with organic and inorganic anions.[4] The comparison of the structural properties of these CT complexes of BO and ET deduced that the origin of the peculiar ability of the BO molecule is ascribed to the presence of ethylenedioxy group as following; the small oxygen atoms exert both multiple CH··O and strong S··S intermolecular atomic contacts which allow the BO units to aggregate by themselves despite of strongly differing acceptor molecules.[2]

SCHEME 1

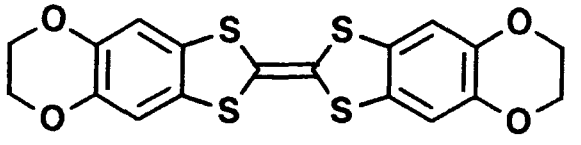

BEDO-DBTTF

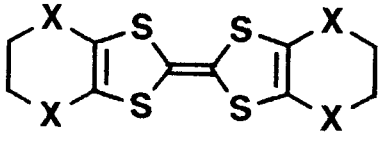

X=S BEDT-TTF(ET)
X=O BEDO-TTF(BO)

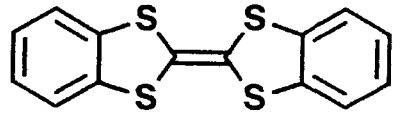

DBTTF

In order to have deep insight into the role of the ethylenedioxy group in formation of conductive CT complexes, we have done comprehensive study on the molecular and electronic structures and CT complex formation of bis(ethylenedioxy)-dibenzotetrathiafulvalene BEDO-DBTTF, the basic block of which; DBTTF, is known as a poor donor in delivering the conductive CT complexes with organic acceptors.[3a,5]

EXPERIMENTAL

Preparation and Purification

The preparation of BEDO-DBTTF is illustrated in Scheme 2. This donor was purified by recrystallization from dimethylformamide. TTF was commercially obtained. All other donors were synthesized according to literatures; BO,[6a] ET,[6b-d] DBTTF,[6e] *etc.*

The following acceptor molecules were synthesized according to the literatures; F_4TCNQ,[7] F_2TCNQ,[7] FTCNQ,[7] CF_3TCNQ,[8a,b] Et_2TCNQ,[7] Me_2TCNQ,[7] TCNNQ,[8b] $(MeO)_2$TCNQ,[7] BTDA-TCNQ,[7] $(EtO)_2$TCNQ,[8a,b] Me_4TCNQ,[8c] TCAQ,[8d] DBDQ,[7] $Q(CN)_2$,[8e] QBr_4,[7] QI_4,[8f] DCNNQ,[8g] DCNQ,[7] Cl_2NNQ,[8h] DTENF,[7] DTNF,[7] TENF,[7] HCBD,[7] and TNBP.[7] While TCNQ, TNAP, DDQ, QCl_4, QF_4, $QCl_2(OH)_2$, $QBr_2(OH)_2$, $Q(OH)_2$, Q, Cl_2NQ, TNF, TCNE, DNBP and TNB were commercially obtained.

All these donors and acceptors were purified by recrystallization and/or gradient sublimation and identified by melting point (Mp) and infra-red (IR) spectra. Elemental analysis was also utilized for identification for the materials synthesized. C_{10}TCNQ and C_{14}TCNQ were kindly supplied by Prof. T.Nakamura and used without further purification. Scheme 3 shows the chemical structures of 40 organic acceptors used in this work, which are classified into five acceptor systems; TCNQ, *p*-quinone, fluorene, percyano and nitrophenyl systems.

CT complexes were prepared by mixing two solutions of BEDO-DBTTF in chlorobenzene or dichloroethane and acceptor in the same solvent or acetonitrile, usually in the mole ratio of donor (D)/acceptor (A) = 1-0.1. The stoichiometry of them was determined solely by the elemental analysis. The stoichiometry of the complex of TCNQ changed by changing solvent. However stoichiometry did not change even if the mole ratios D/A of about 0.2, 1.0, and 5.0 were employed for the preparation of CT complexes with F_4TCNQ, F_2TCNQ and BTDA-TCNQ. The

highly conductive complexes of Me_2TCNQ and $(MeO)_2TCNQ$ were obtained by direct mixing of the solutions while the insulating single crystals by diffusion method. With the other acceptors, neither single crystals nor other stoichiometries other than those described below were successfully obtained, though not so extensive examinations have been performed for complex formation concerning about concentration, solvent, temperature, *etc.*

SCHEME 2 Preparation of BEDO-DBTTF

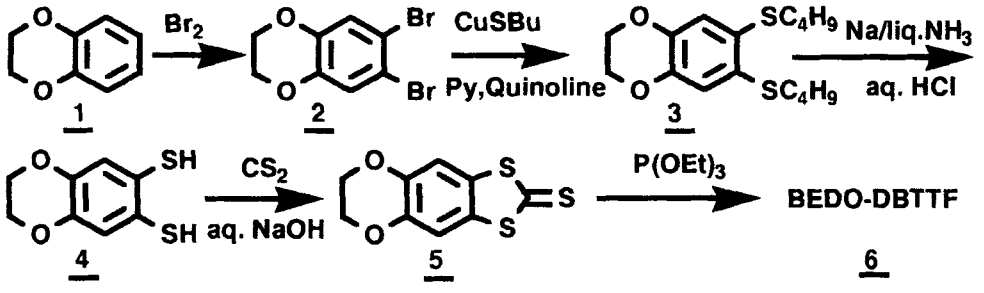

1,2-Dibromo-4,5-ethylenedioxybenzene (2). According to the same method of 4,5-dibromoveratrole,[9] 2 was synthesized by treating 1,4-benzodioxane (1) (30.7g, 225 mmol) with bromine (75g, 470 mmol) in chloroform solution at 0°C over 5 h. Yield 94%; colorless plate; Mp 135-136°C; ^{1}HNMR($CDCl_3$, TMS) δ=4.23(4H,s), 7.12(2H,s); MS m/e 294(M^+).

1,2-Bis(butylthio)-4,5-ethylenedioxybenzene (3). Cuprous n-butylmercaptide was prepared as the same procedure of R.Adams *et al.*[10] 2 (29.4g, 100 mmol) was stirred and refluxed for 3 h at 150°C with fresh cuprous n-butylmercaptide (38.2g, 250 mmol) in a mixture of dry quinoline (100 ml) and dry pyridine (10 ml) under N_2. After cooling to *ca.* 100°C, the reaction solution was poured into a stirred mixture of ice (250g) and conc. HCl (150 ml); occasional stirring was continued for about 2 h. The aqueous part was discarded by decantation and the dark brown, gummy residue was extracted three times with dichloromethane. The dichloromethane extract was washed twice with 10% HCl, once with water, twice with conc. ammonium hydroxide, and with water again. The organic solution was dried over anhydrous magnesium sulfate and the filtrate was evaporated under reduced pressure. The residue was developed on a silica gel chromatography with a mixture of dichloromethane and hexane, giving a brown oily product. Yield 90%; ^{1}HNMR($CDCl_3$) δ=0.92(6H,t), 1.45(4H,m), 1.62(4H,m), 2.83(4H,t), 4.23(4H,s), 6.84(2H,s); MS m/e 312(M^+).

4,5-Ethylenedioxy-1,2-benzenedithiol (4). Compound 4 was prepared in the same manner as *o*-benzenedithiol.[11] 3 (16.4g, 52.4 mmol) was dissolved in 105 ml of liquid NH_3 with vigorous stirring at *ca.*-70°C under N_2, and subsequently granular sodium (6.03g, 262.2 mmol) was

was added in small pieces. After the reaction was maintained for 1 h, excess NH_4Cl was added to stop a progress of the reaction. After complete color fading of the solution, NH_3 was removed by passing a stream of N_2 and warming the solution to room temperature (RT). The remaining white solid was dissolved carefully in 10% aq. NaOH. The alkaline solution was extracted with diethylether and the ether extracts were discarded. The acidification of the alkaline solution by 6N HCl precipitated 4 as a pale yellow solid. Yield 90%; Mp 90–94°C; ^{1}HNMR($CDCl_3$) δ=3.63(2H,s), 4.22(4H,s), 6.94(2H,s); MS m/e 200(M^+).

5,6-Ethylenedioxybenzo-1,3-dithiol-2-thione (5). After 4 (10.0g, 50mmol) was dissolved in 125 ml of 1 mmol·dm^{-3} NaOH solution, 15ml (250 mmol) of carbon disulfide was added to the alkaline solution. Reflux for 3h gave 5 as a yellow solid. Yield 96%; Mp 209–210°C; ^{1}HNMR($CDCl_3$) δ=4.30(4H,s), 6.98(2H,s); MS m/e 242(M^+).

BEDO-DBTTF (6). A mixture of 5 (10.9g, 45 mmol) and triethyl phosphite (66.2 ml, 382 mmol) in 66 ml of benzene was refluxed for 5 h under N_2 to give orange precipitate which was filtered off and washed with methanol and dichloromethane. Orange needle; Mp>350°C; MS m/e 420(M^+); Found:C,51.43; H,2.83%. Calcd: C,51.41; H,2.87%.

Measurements

Melting points were not corrected. Cyclic voltammetric measurements were performed in 0.1M solutions of tetrabutylammonium(TBA)·BF_4 in acetonitrile with Pt electrodes *vs.* SCE at 10~20mV/sec at 20-22°C. The optical measurements were carried out on Perkin-Elmer 1600 Series FT-IR (resolution 4 cm^{-1}) for IR and near-IR (NIR) regions (400~7800 cm^{-1}) in KBr and on SHIMADZU UV-3100 spectrometer for UV-VIS-NIR region (3800~42000 cm^{-1}) in KBr or solution. The d.c. conductivities were measured based on a standard four- or two-probe technique attaching gold wires (15μmϕ) on samples by gold paint (Tokuriki 8560-1A).

The intensity data of the structural analysis were collected on automatic four circle diffractometer at RT. The structures were solved by direct methods. The refinements of structures were performed by full matrix least squares method. The crystal, data collection and refinement parameters are summarized in Table I. The parameters were refined adopting anisotropic temperature factors for non-hydrogen atoms. The positions of hydrogen atoms of the benzene rings of BEDO-DBTTF in $(MeO)_2$TCNQ complex were determined by differential synthesis. Other hydrogen atoms were determined by fixing C-H bond length of 0.96Å with SP^3 or SP^2 configuration. They were refined with isotropic temperature factors. The atomic coordinates are summarized in the Appendix.

SCHEME 3 Acceptor molecules used in this work

1 TCNQ system

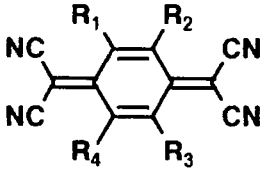

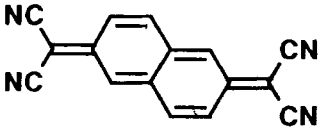

TNAP

R_1,R_2,R_3,R_4=F: F_4TCNQ
R_1,R_3=F R_2,R_4=H: F_2TCNQ
R_1=F R_2,R_3,R_4=H: FTCNQ
R_1,R_2,R_3,R_4=H: TCNQ
R_1=CF_3 R_2,R_3,R_4=H: CF_3TCNQ
R_1,R_3=CH_3 R_2,R_4=H: Me_2TCNQ
R_1,R_3=C_2H_5 R_2,R_4=H: Et_2TCNQ
R_1,R_3=OCH_3 R_2,R_4=H: $(MeO)_2TCNQ$
R_1,R_3=OC_2H_5 R_2,R_4=H: $(EtO)_2TCNQ$
R_1=C_nH_{2n+1} R_2,R_3,R_4=H: C_nTCNQ(n=10,14)
R_1,R_2=$CH(CH)_2CH$ R_3,R_4=H: TCNNQ
R_1R_2,R_3R_4=NSN: BTDA-TCNQ
R_1,R_2,R_3,R_4=CH_3: Me_4TCNQ
R_1R_2,R_3R_4=$CH(CH)_2CH$: TCAQ

2 p-Quinone system

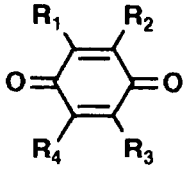

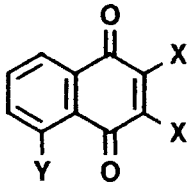

R_1,R_2=CN R_3,R_4=Cl: DDQ
R_1,R_2=CN R_3,R_4=Br: DBDQ
R_1,R_2=CN R_3,R_4=H: $Q(CN)_2$
R_1,R_2,R_3,R_4=F: QF_4
R_1,R_2,R_3,R_4=Cl: QCl_4
R_1,R_2,R_3,R_4=Br: QBr_4
R_1,R_2,R_3,R_4=I: QI_4
R_1,R_2,R_3,R_4=H: Q
R_1,R_3=OH R_2,R_4=Cl: $QCl_2(OH)_2$
R_1,R_3=OH R_2,R_4=Br: $QBr_2(OH)_2$
R_1,R_3=OH R_2,R_4=H: $Q(OH)_2$
X=Cl Y=H: Cl_2NQ
X=Cl Y=NO_2: Cl_2NNQ
X=CN Y=H: DCNQ
X=CN Y=NO_2: DCNNQ

3 Fluorene system

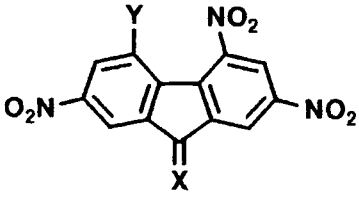

X=O Y=H: TNF
X=O Y=NO_2: TENF
X=$C(CN)_2$ Y=H: DTNF
X=$C(CN)_2$ Y=NO_2: DTENF

4 Percyano system

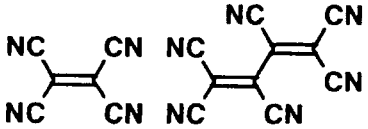

TCNE HCBD

5 Nitrophenyl system

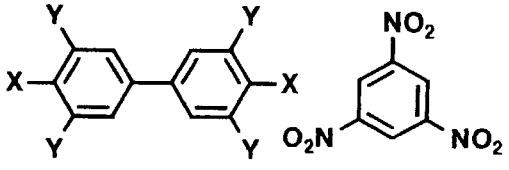

X=NO_2 Y=H: DNBP
X=OH Y=NO_2: TNBP

TNB

TABLE I Crystal data, data collection and reduction parameters for neutral BEDO-DBTTF and 1:1 complexes of BEDO-DBTTF·Me_2TCNQ (18b) and BEDO-DBTTF·$(MeO)_2$TCNQ (20b).

	neutral BEDO-DBTTF	BEDO-DBTTF·Me_2TCNQ 1:1 (18b)	BEDO-DBTTF·$(MeO)_2$TCNQ 1:1 (20b)
Formula	$C_{18}H_{12}O_4S_4$	$C_{32}H_{20}N_4O_4S_4$	$C_{32}H_{20}N_4O_6S_4$
Formula wt	420.57	652.81	684.81
Crystal dimension	0.30x0.10x0.10 mm^3	0.34x0.08x0.06 mm^3	0.50x0.08x0.05 mm^3
Crystal system	orthorhombic	monoclinic	monoclinic
Space group	$P2_12_12_1$	$P2_1/a$	$P2_1/a$
a/	16.131(4)	19.685(2)	16.975(7)
b/	25.577(7)	7.293(1)	8.437(4)
c/	4.003(2)	9.896(1)	10.465(4)
β/deg	90	94.611(8)	93.85(1)
V/ ^{3}	1652(1)	1416.2(2)	1495(1)
Z	4	2	2
D_{calc}, g/cm^3	1.69	1.53	1.52
D_{obs}, g/cm^3		1.51	1.49
Diffractometer	Mac Science MXC18HF	Mac Science MXC18K	Mac Science MXC^x
Radiation	Mo Kα	Mo Kα	Mo Kα
Scan mode	$2\theta\omega$	$2\theta\omega$	$2\theta\omega$
$2\theta_{max}$	55°	55°	55°
No. of intensity meas.	2372	3245	3440
Criterion for obsd. reflection	$\|F_o\| \geqq 3\sigma\|F_o\|$	$\|F_o\| \geqq 6\sigma\|F_o\|$	$\|F_o\| \geqq 6\sigma\|F_o\|$
Reflections used in L.S.	1675	1537	1649
No. of refined parameters	235	218	236
R	0.0486	0.0414	0.0523
Rw	0.0543	0.0552	0.0677

RESULTS AND DISCUSSION

Structure and Properties of BEDO-DBTTF

Molecular Structures and Molecular Orbitals

The molecular and crystal structures of BEDO-DBTTF are shown in Figure 1. Bond lengths (Å) and angles (degree) are presented in Figure 1a. The molecule is bent as a boat shape (Figure 1b) as those observed in BO and ET molecules. The dihedral angles between the central tetrathioethylene plane and the outer residual benzenedithio planes are 176.4° and 172.1°, indicating that a BEDO-DBTTF molecule is

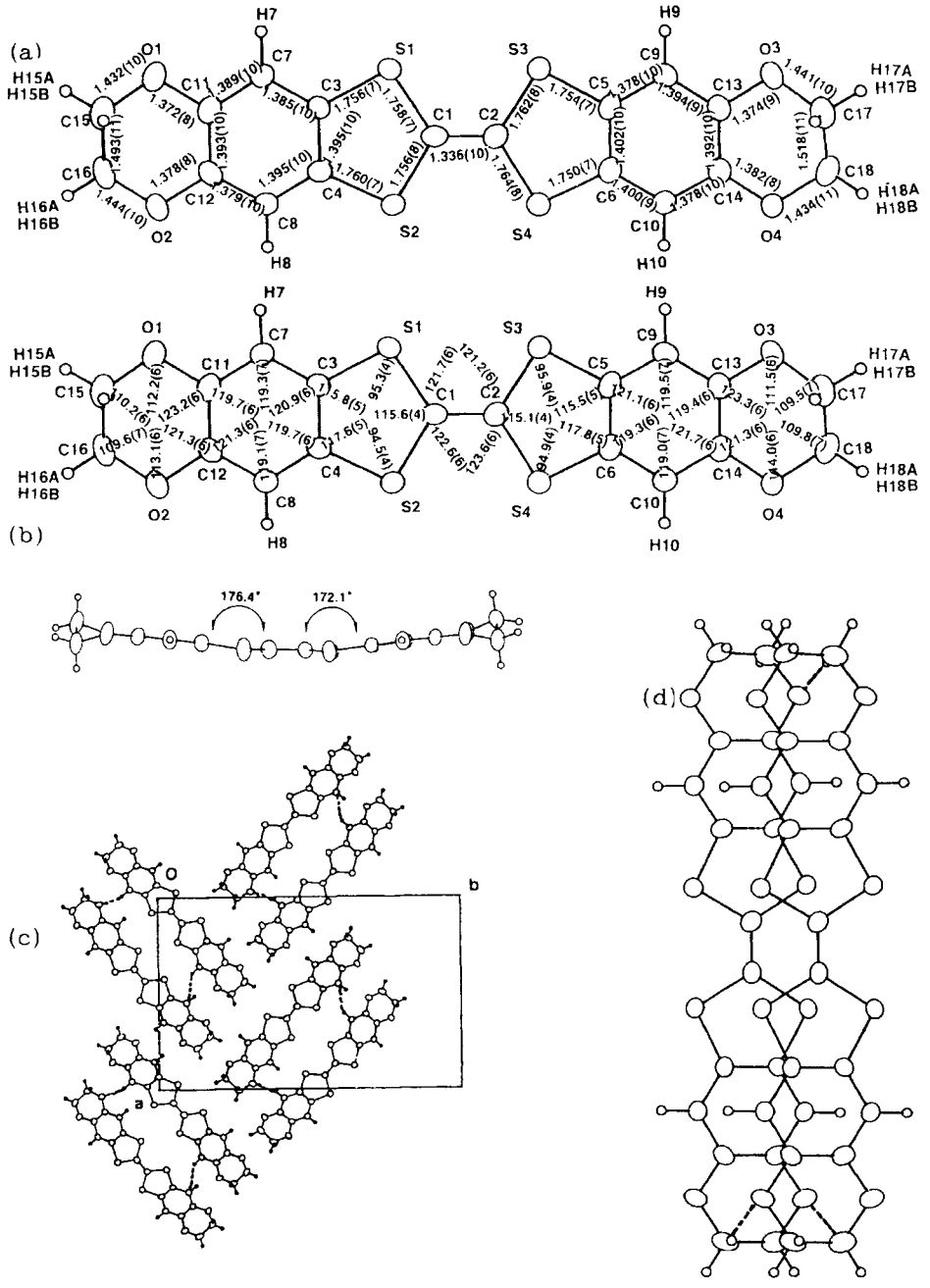

FIGURE 1 Molecular and crystal structures of BEDO-DBTTF: (a) bond lengths (Å) and angles (degree); (b) dihedral angles (degree) between the central tetrathioethylene moiety and residual benzenedithio planes; (c) stacking pattern; intermolecular short contacts are shown by dotted lines; and (d) overlapping mode of the molecule viewed on the molecule.

more planar than ET (165.3°, 167.7°) and BO (158.5°, 165.4°). The terminal ethylene groups are ordered with eclipsed conformation. Two BEDO-DBTTF molecules form a pair along side-by-side direction and pairs stack along the c-axis (Figure 1c) with averaged interplanar distance of 3.60Å, which is the same as that of DBTTF crystals.[5f] The overlapping mode is slipped stacking only along their transverse directions as depicted in Figure 1d.

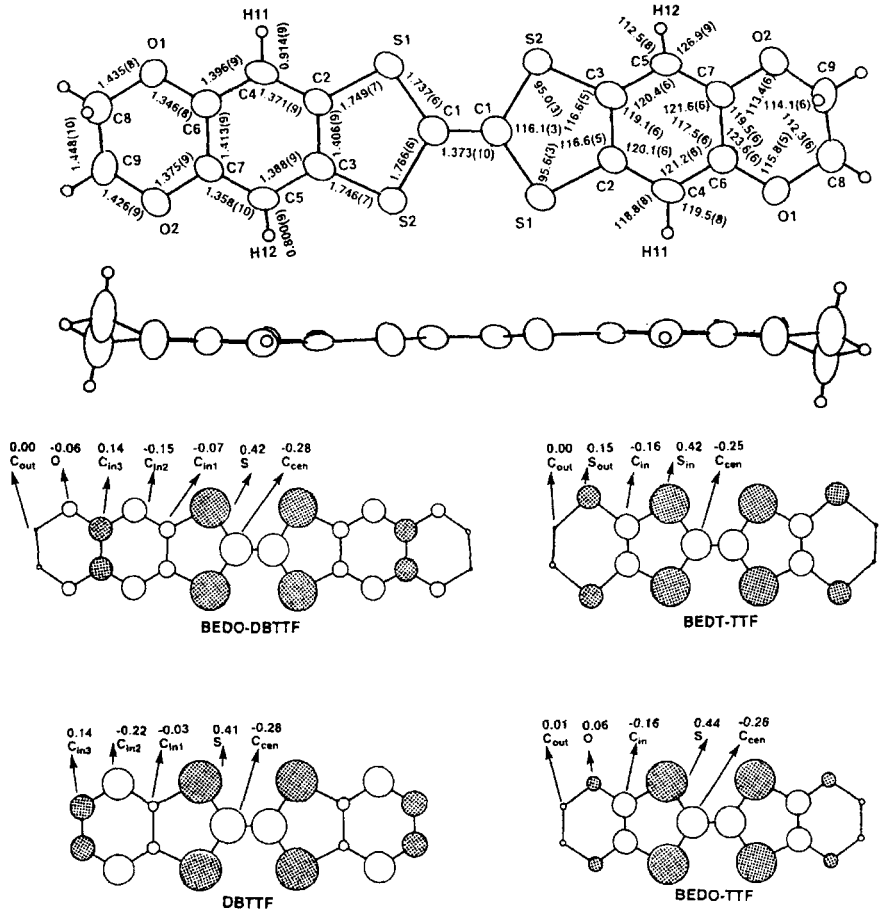

FIGURE 2 Bond lengths (Å) and angles (degree) of BEDO-DBTTF in the 1:1 $(MeO)_2TCNQ$ complex and calculated HOMO coefficients of BEDO-DBTTF, ET, DBTTF and BO molecules based on the molecular structures of donor molecules in neutral CT complexes (see text). The magnitude of the coefficient is shown by the radius of the circle.

The BEDO–DBTTF molecules become almost flat except the terminal ethylene groups upon formation of CT complex with $(MeO)_2TCNQ$ (Figure 2) or Me_2TCNQ (*vide infra*). This kind of flattening nature of donor molecules is a rather common feature among the bisethylene–dichalcogeno derivatives of TTF.

For molecular orbital calculation by the extended Hückel method we adopted the molecular structures of donor molecules in the CT complexes having neutral ground state; namely 1:1 $(MeO)_2TCNQ$ complex for BEDO–DBTTF, 1:2 $Q(OH)_2$ complex[2] for BO, monoclinic 1:1 TCNQ complex[3b] for ET, and 1:1 TCNQ complex[5a] for DBTTF. It is seen that the geometry of the central TTF moieties of four kinds of donor molecules is very similar to each other. The HOMO coefficients of the central tetrathioethylene group of BEDO–DBTTF are very similar to those of BO, ET and DBTTF but those of the outer ethylene carbons of TTF moiety are less than half in absolute value than those of ET and BO but more than twice of those of DBTTF (Figure 2). Though the sign is different, the HOMO coefficients of oxygen atoms are the same in magnitude between BEDO–DBTTF and BO. It is worth noting that the symmetry of HOMO of BEDO–DBTTF is different from that of BO or ET due to the presence of benzene moiety between TTF and ethylenedioxy groups.

Table II compares the molecular dimensions of BO, ET and BEDO–DBTTF molecules in the neutral CT complexes, where a, b, c and d are the distances between carbon atoms of outer ethylene groups, between outer chalcogen atoms, between inner chalcogen atoms, and between hydrogen atoms on the benzene ring as shown at the footnote of Table II, respectively. The most pronounced features of the molecular dimensions of BEDO–DBTTF are both the length of the molecular long axis; a, and the width; d. The length a of a BEDO–DBTTF molecule is 1.3~1.6 times those of ET and BO. So the total area of molecular plane of BEDO–DBTTF is quite much bigger than those of ET and BO. It has been known that a molecule having an extended π-system is able to provide organic metals of self-aggregated stacking with considerably small degree of CT (γ) as exemplified by complexes of TTP analogs[12] and phthalocyanine complexes[13] ($\gamma \geq 0.3$), though the conventional organic metal of TTF·TCNQ system bears $1 > \gamma \geq 0.5$. So it may be possible that BEDO–DBTTF provides self-aggregated partial CT state with weaker

TABLE II Molecular dimensions of BEDO-TTF, BEDT-TTF and BEDO-DBTTF molecules in neutral CT complexes[1].

	a/ Å	b / Å	c / Å	d / Å	b/c
BEDO-TTF	10.1	2.90	2.99	-----	0.97
BEDT-TTF	11.8	3.54	2.96	-----	1.20
BEDO-DBTTF	16.0	2.84	2.97	4.48	0.96

1) BO in $(BEDO\text{-}TTF)[Q(OH)_2]_2$[2], ET in monoclinic BEDT-TTF·TCNQ[3b] and BEDO-DBTTF in BEDO-DBTTF·$(MeO)_2$TCNQ. The a~d values are the distances as indicated below for BEDO-DBTTF as an example.

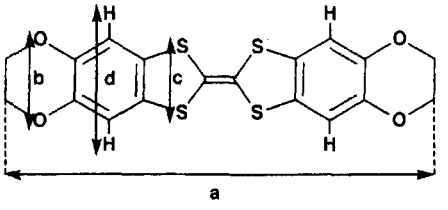

acceptors than expected for the conventional TTF·TCNQ system.

The easy accessibility of partial CT state is also expected for BEDO-DBTTF owing to the presence of ethylenedioxy group as is observed in the BO system.[2] The HOMO coefficient of outer chalcogen atoms of BEDO-DBTTF or BO is small compared to that of ET. Nevertheless, numbers of hydrogen bond-like atomic contacts between ethylene groups and oxygen atoms are expected and that would enhance the stable self-aggregation state even with small γ. These features are the advantageous molecular nature of BEDO-DBTTF for achieving metallic conductivity.

The b is a little shorter than the c in BO. This molecular geometry exerts the strong peculiarity in the case of BO complexes, namely strong side-by-side intermolecular interactions by the aid of $S_{in}\cdot\cdot S_{in}$ atomic contacts are realized by small b/c, where S_{in} is inner sulfur atom. While in the ET case, the b is much larger than the c, so the side-by-side interaction is accomplished mainly by less efficient $S_{in}\cdot\cdot S_{out}$ contacts. Since the coefficient of HOMO on the outer chalcogen atoms is considerably small compared with that of S_{in} (S_{in}=0.44, S_{out}= 0.15 for ET), the $S_{in}\cdot\cdot S_{in}$ contacts are very effective in terms of intermolecular transfer interactions in contrast with the $S_{in}\cdot\cdot S_{out}$ contacts for TTF analogs. Although the coefficients of HOMO of chalcogen atoms are not much different between BO and BEDO-DBTTF, the d seems to be critical for the latter to gain sufficient side-by-side

interaction. The hydrogen atoms of benzene rings may prohibit the proximate approach of BEDO–DBTTF molecules along the side-by-side direction and prevent such $S_{in}\cdot\cdot S_{in}$ and $S_{in}\cdot\cdot O$ atomic contacts since the d is very much bigger than both b and c. In the crystal of neutral BEDO–DBTTF molecules, significantly short contacts less than the van der Waals (vdW) sum[14] are observed at C(9)··H(7) (2.85 *vs.* 2.90Å) and O(1)··H(9) (2.65 *vs.* 2.72Å), where H(7) and H(9) are the hydrogen atoms of benzene rings (Figure 1c). Also along the oblique direction, very short contacts are observed between oxygen atoms and ethylene hydrogen atoms; O(1)··H(15B) (2.67Å), O(2)··H(16B) (2.65Å) and O(3)··H(17A) (2.43Å) (Figure 1d). However, there are no short S··S atomic contacts along any directions; the observed atomic contacts of 3.78~3.90Å are larger than the vdW sum of 3.60Å. That is a quite different feature from those in ET and BO crystals and this is the disadvantageous molecular feature of BEDO–DBTTF for the increment of the transverse transfer interaction.

Therefore on the basis of the sterical and orbital considerations, BEDO–DBTTF is expected to afford self-aggregated complex with partial CT ground state as BO does, but to give lower dimensional conductors than BO does.

Redox Property

Table III compares the melting points, redox potentials (E(D)), CT band energies of TNB complexes ($h\nu_{CT}$(D·TNB)), and absorption peak energies of neutral and cation molecules in solution of BEDO–DBTTF, ET, BO and DBTTF. The donor molecules are arranged in the decreasing order of the first redox potential (E^1(D) = average value of the oxidation and reduction peak-potentials for $D^0 \rightleftarrows D^{+1}$) or $h\nu_{CT}$(D·TNB). It is recognized that the donor ability of BEDO–DBTTF is much better than that of DBTTF based on its electronic structure, *viz.* the E^1(D) value of BEDO–DBTTF which is comparable to that of ET, is enhanced by 0.12 V from that of DBTTF and locates at the middle of those of DBTTF and BO. The same tendency was observed in the CT absorption energy of the TNB complex in $CHCl_3$; the CT absorption of BEDO–DBTTF·TNB complex exhibits a red-shift of 1.5×10^3 cm^{-1} (0.19 eV) compared to that of DBTTF·TNB complex.

It has been known that the unsubstituted TTF and TSF molecules

among the tetrachalcogenafulvalene derivatives show big deviation from the linear relation between redox potentials and adiabatic ionization potentials (I^{ad}) of them.[15] Unexpectedly high I^{ad}'s have been observed for these two donor molecules. While, a plot of $E^1(D)$ *vs.* vertical *ionization potentials* $(I^V)^2$ *or* $E^1(D)$ *vs.* $h\nu_{CT}(D^{\bullet}TNB)$ (Figure 3) exhibits rather excellent linear relation. This indicates that either $h\nu_{CT}(D^{\bullet}TNB)$ or $E^1(D)$ is an appropriate parameter for a measure of the I^V of D. The fact that BEDO–DBTTF locates near the line in Figure 3 shows that both its $h\nu_{CT}(D^{\bullet}TNB)$ and $E^1(D)$ values are experimentally reliable ones. While either $h\nu_{CT}(D^{\bullet}TNB)$ or $E^1(D)$ values of TTF and TSF include uncertainty. At a same time, it also indicates that the observed I^{ad}'s of

TABLE III Melting points, redox potentials, charge transfer transition energies of TNB complexes in solution ($h\nu_{CT}(D^{\bullet}TNB)$) and absorption energies of neutral and cation radical molecules in solution of DBTTF, BEDT–TTF, BEDO–DBTTF, BEDO–TTF and TTF.

TTF	Mp (°C)	redox potential[1] (V vs. SCE) $E^1(D)$	$E^2(D)$	$\triangle E^{12}$	$h\nu_{CT}$[2] (D·TNB) $\times 10^3 cm^{-1}$	absorption[3] $\times 10^3 cm^{-1}$ neutral	cation
DBTTF	238-239	0.63	0.95	0.32	17.3	23.1 29.2(sh) 31.9	15.8 20.2(weak) 22.8, 24.0 32.9, 33.8
BEDT -TTF	244(dec)	0.53	0.78	0.25	16.1	21.8 28.6 30.9	10.4 17.4(sh) 20.8, 22.0 29.0
BEDO-DBTTF	>350(dec)	0.51	0.80	0.29	15.8	22.5(sh) 30.8	12.2 18.9(sh) 22.0, 23.1 31.5
BEDO -TTF	178(dec)	0.43	0.69	0.26	15.0	19.3 29.3 31.4	10.6 16.5(weak) 20.4, 21.7 29.8, 31.8
TTF	120-123	0.37	0.73	0.38	15.4	22.3 26.8(sh) 31.9	17.3 20.0(sh) 23.0, 30.3 31.4

1) Average value of the oxidation and reduction peak-potentials for $D^0 \rightleftharpoons D^{+1}$ or $D^{+1} \rightleftharpoons D^{+2}$; *vs.* SCE, Pt electrode, CH_3CN, 0.1M $TBA^{\bullet}BF_4$, 20~22°C, 10~20 mV/sec. 2) TNB complex in $CHCl_3$ at 20~22°C. 3) $CHCl_3$ solutions for neutral molecules. 4) Methanol solutions of $DBTTF^{\bullet}Br_2^{\bullet}H_2O$,[16] BEDT–TTF·Br·$H_2O$, BEDO–$DBTTF^{\bullet}Br_{2.1}^{\bullet}(H_2O)_{0.8}$,[16] BEDO–$TTF_2^{\bullet}Br^{\bullet}(H_2O)_3$ and $(TTF)_3(BF_4)_2$.

both TTF and TSF include some experimental errors and need to be reexamined. Hence we will not use the I^{ad} values. Also no vertical ones are used since they are not available for all of the TTF derivatives in this study. Later we will see that which parameter, *i.e.* $E^1(D)$ or $h\nu_{CT}(D^{\bullet}TNB)$, is more appropriate for a measure of donor strength.

The difference of the first and second redox potentials ($\Delta E^{12} = E^1(D)-E^2(D)$), which is a measure of the electron correlation energy (U) in a molecule,[17] of BEDO–DBTTF is smaller than that of DBTTF by 0.03 V. However, the ΔE^{12} value is larger than those of BO and ET by 0.03~0.04 V even though the molecular length of BEDO–DBTTF is 1.3~1.6 times those of BO or ET. This fact contradicts with the usual observation that the larger the molecular size, the smaller the U value among a series of molecules structurally related,[18] for example, the extended TTF analogs such as TTP compounds[12] or BDNT compound[19] have very small U. From this point of view, BEDO–DBTTF is expected to afford less conductive materials than BO.

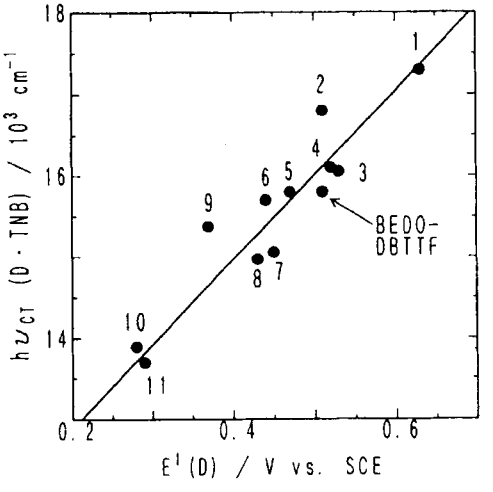

FIGURE 3 A plot of charge transfer band energy ($h\nu_{CT}(D^{\bullet}TNB)$) *vs.* first redox potential ($E^1(D)$) of several TTF derivatives (1:DBTTF, 2:TSF, 3:BEDT–TTF, 4:TTC_1–TTF, 5:TSC_1–TTF, 6:EDT–TTF, 7:TMTSF, 8:BEDO–TTF, 9:TTF, 10:TMTTF and 11:HMTTF. The line is a least squares fit excluding TTF and TSF.

Absorption Spectra in Solution

The absorption spectra of neutral donor molecules in Table III are similar to each other. They have very weak HOMO–LUMO absorption at

19.3, 21.8, *ca.* 22.5(sh) and 23.1x10^3 cm^{-1} for BO, ET, BEDO-DBTTF and DBTTF, respectively, as shown in Figure 4. A strong broad absorption appears at around 30~31x10^3 cm^{-1} which usually hides a medium absorption at around 29x10^3 cm^{-1}.

The cation radicals in solution show two different patterns of absorption spectra depending on whether the donor molecules have extended π-system containing chalcogen atoms or not. In the latter system (DBTTF (Figure 4d), TMTTF, TTF, *etc.*) cation molecules show the lowest energy absorption (termed as C-band) at 15~17x10^3 cm^{-1}, a weak one at 19~20x10^3 cm^{-1} (D-band), and rather strong one with usually double peaks at 22~25x10^3 cm^{-1} (E-band). While the former system (BEDO-DBTTF (Figure 4a), BO (Figure 4b), ET (Figure 4c), EDT-TTF, TTC_1-TTF, *etc.*) exhibits the C band at considerably low energy side (10~13x10^3 cm^{-1}), the D band at a little lower side (17~19x10^3 cm^{-1}) and the E- band at the same positions (20~23x10^3 cm^{-1}) as the latter system. The strong bands of $(BO)_2Br(H_2O)_3$ above 30x10^3 cm^{-1} is ascribable to neutral BO molecules.

It has been reported that the band at around 10x10^3 cm^{-1} (C-band) of ET^+ in solution or solid is accounted for a dimer of monocation radicals or a doubly occupied site which is related to U.[20] This assignment was based on the analogy to the fact that TTF cation dimer showed the lowest-energy absorption at considerably low energy side (12x10^3 for intra-, 15x10^3 cm^{-1} for interdimer in solid, 14x10^3 cm^{-1} in solution) compared to that of monomer (19x10^3 in solid, 17x10^3 cm^{-1} in solution).[21] However, it is evident that the C-band is not due to the cation dimer but to the intramolecular origin from the following reasons.

1) The C-band follows the Beer's law in the concentration range of 1x 10^{-6}~4x10^{-5} mol/dm^3 for ET and BO. 2) A KBr disk of $(ET)_2[Pt(dto)_2]$ complex, where ET cation dimer is nearly isolated by the dianion molecules of Pt(dithiooxalate(dto))$_2$, shows not only the C-band at 12x10^3 cm^{-1} but also a band at 8x10^3 cm^{-1} (B-band).[22] In solution only the B band disappears, while the C band remains at 10x10^3 cm^{-1}. A similar spectral change was observed in ET·Br and BO·I_3 salt (see Figure 4b, 4c). The B and C-bands appear at 5.5x10^3 and 10.0x10^3 cm^{-1} in solid ET·Br, respectively. While the B band appears 7~10x10^3 cm^{-1} (7.8x10^3 cm^{-1} for intra- and 9.8x10^3 cm^{-1} for interdimer) and C-band

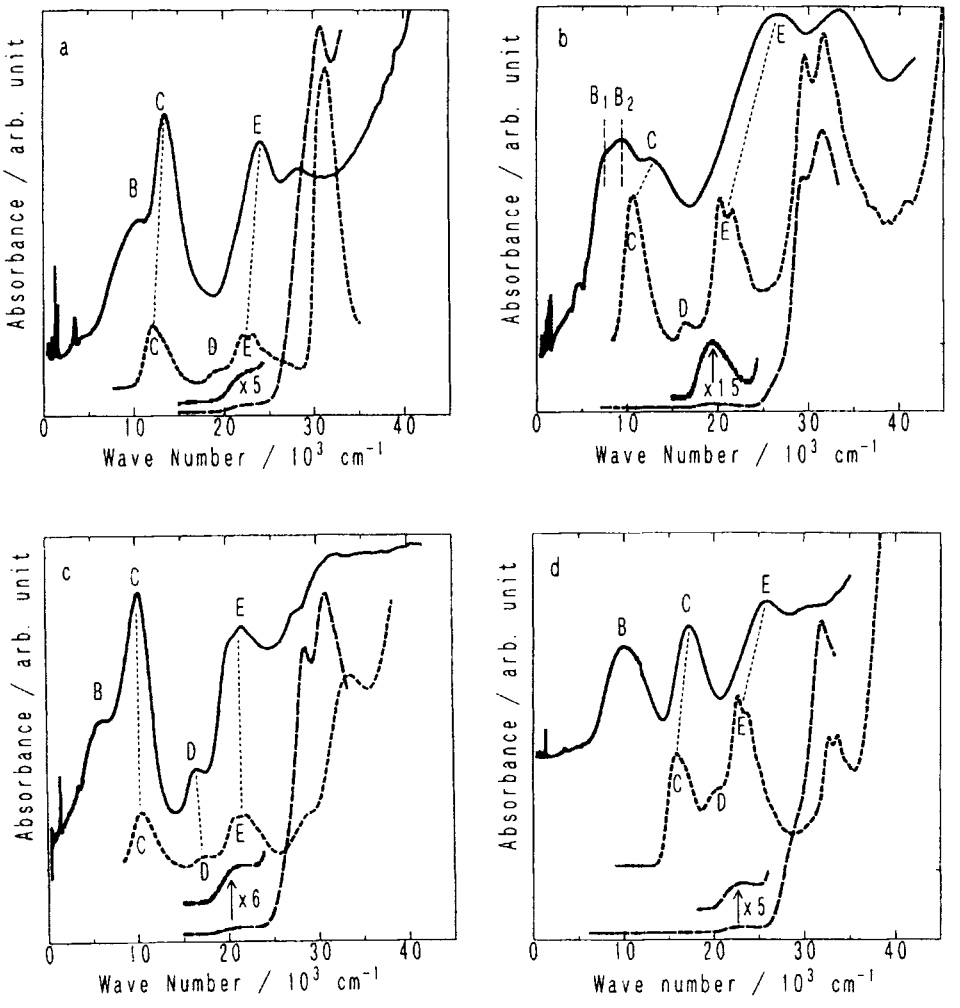

FIGURE 4 Absorption spectra of neutral (broken line, in $CHCl_3$) and cation (dotted line in methanol; solid line in KBr) molecules of (a) BEDO–DBTTF, (b) BEDO–TTF, (c) BEDT–TTF and (d) DBTTF. Cation molecules are those in BEDO–DBTTF·$Br_{2.1}$·$(H_2O)_8$,[16] $(BEDO–TTF)_2Br(H_2O)_3$ (in methanol), BEDO–TTF·I_3 (in KBr), BEDT–TTF·Br and DBTTF·Br_2·H_2O.[16]

at 12~ 13x10^3 cm^{-1} in solid BO·I_3.[23] Therefore, the B-band is the intermolecular transition associated with the effective U but the C-band is not. 3) The C-band is clearly observed even for complexes of γ=0.5, where the intensity is expected to vanish theoretically, if it is intermolecular origin.[24] 4) Absorptions polarized along the long axis of the ET molecule are observed at 9.7 (C-band), 16.0 (D), 20.0 (E) and 11.4 (C), 16.1 (D) and 19.9x10^3 cm^{-1} (E) for α-$(ET)_2I_3$ and κ-$(ET)_2Cu$

$(NCS)_2$, respectively.[25] Accordingly we conclude that the C-band is the lowest intramolecular transition, which is polarized along the long axis of TTF derivatives, originated most likely from second HOMO to HOMO. It should be noted that the B-band of BEDO-DBTTF salt appears at higher energy side than that of ET or BO salt and almost at the same position that of DBTTF salt. This fact indicates that the effective U value of the BEDO-DBTTF materials is larger than those of ET and BO materials and comparable to that of the DBTTF ones.

Prediction of Ionicity of CT Complex

According to the most simplified theory by McConnell, Hoffman and Metzger,[26] the boundary of the ionicity of a CT complex crystal is represented by a formula;

$$I_D - E_A = M \quad (1),$$

where I_D, E_A and M are ionization potential of D, electron affinity of A and Madelung energy of the crystal, respectively. Considering the effects of the transfer interaction,[27] ionicity dependence of M,[28] stacking pattern dependence of M,[28] size and shape effect on M,[29] *etc.*, there appears a narrow region of partial CT state neighboring the fully ionic region. As a consequence conventional 1:1 CT complexes, $D^{+\gamma}A^{-\gamma}$ (usually $0 \leq \gamma \leq 1$), are classified into three groups, namely I) neutral insulator ($0 \leq \gamma < \gamma_c$), II) partially ionic conductor ($\gamma_c \leq \gamma < 1$) and III) fully ionic insulator ($\gamma = 1$). The threshold value γ_c is specific to particular DA system, below which the system prefers to form alternating stack than the segregated one and so is an insulator. It is known that a diagram of structurally related acceptor molecules on the vertical line and structurally related donor molecules on the horizontal line according to their redox properties can discriminate the three regions of a particular DA system.[30] Of course, there are many CT complexes having partial ionicity but insulating owing to the inconvenient stacking manner and/or electronic structure for conduction (*vide infra*). Also there are very few 1:1 CT complexes of high conductivity with fully ionic nature in which effective U may become accidentally smaller than the band width.[31] We predict the ionicity of BEDO-DBTTF CT complexes by adopting the partial ionicity regime of conventional 1:1 TTF·TCNQ system proposed by Saito and Ferraris,[30]

$$-0.02 \leq \Delta E(DA) \leq 0.34 \text{ V} \quad (2).$$

The $\Delta E(DA)$ ($=E^1(D) - E^1(A)$) is a redox version of ($I_D - E_A$). The 1:1 CT complexes of TTF·TCNQ system of low-dimensional nature are fully ionic insulators in the region $\Delta E(DA) < -0.02$ V, and those in the region $\Delta(DA) > 0.34$ V prefer the alternating stacking insulating state with small γ (<0.5).

CT Complexes

Acceptor Strength

The data of the complexes are summarized in Table IV. The first column shows the entry number which represents both acceptor molecule and complex of the corresponding acceptor. The second column includes the data of acceptors used; the acceptor molecule, its first redox potential ($E^1(A)$ = average value of the reduction and oxidation peak-potentials for $A^0 \rightleftharpoons A^{-1}$) and CT band energy of pyrene complex in $CHCl_3$ ($h\nu_{CT}$(pyrene·A)). The complexes are arranged according to the redox potentials of acceptor molecules.

A plot of $h\nu_{CT}$(pyrene·A) against $E^1(A)$ in Figure 5 gave different straight lines with different acceptor systems but with similar slope. The TCNQ system (□) includes 16 acceptors among which bulky Me_4TCNQ(28) and TCAQ(33) are known to exhibit two-electron reduction process at $E^1(A)$ and deviate from the line of TCNQ system in Figure 5 considerably. The *p*-quinone system (○) includes 15 acceptors. QF_4(23), $QBr_2(OH)_2$(29), $QCl_2(OH)_2$(30) and Q(37) are out of the line. The $E^1(A)$ data of dihydroxy-*p*-benzoquinones(29, 30) deviate from the line because they are just the peak potentials of the process of $A^0 \rightarrow A^{-1}$. Reasonable redox potentials of 29 and 30 can be estimated as *ca.* −0.29 and −0.28 V *vs.* SCE, respectively, assuming that those are on the line of *p*-quinone system as indicated by arrow in Figure 5. It is not clear why 23 and 37 deviate from the line. $Q(OH)_2$(34) did not give clear CT band, so it is not possible to estimate its redox potential. The percyano (▲; 1, 10) and fluorene acceptors (●; 12, 25, 31, 36) locate between the lines of TCNQ and *p*-quinone systems. The nitrophenyl acceptors 38 and 39 do not give distinct CT band, so they are not included in Figure 5.

The fact that a different line corresponds to different acceptor system in Figure 5 is mainly attributable to the dependence of

solvation energy term, $\Delta E(solv)$, in $E^1(A)$ on different system;[18] $E^1(A) = E_A - \Delta E(solv) - \phi_{Hg} - E^{\emptyset}(Hg:Hg^{2+})$, where ϕ_{Hg} is the work function of Hg and $E^{\emptyset}(Hg:Hg^{2+})$ is the electrode potential of SCE against the hydrogen electrode. From this point, the $h\nu_{CT}$(pyrene·A) value which

TABLE IV Color, shape, stoichiometry, optical, conductivity and ionicity data of BEDO–DBTTF complexes together with redox potentials ($E_1(A)$) and charge transfer transition energies of pyrene complexes ($h\nu_{CT}$(pyrene·A)) of acceptor molecules.

	Acceptor Molecule		BEDO-DBTTF Complex							
	$E_1(A)$[1] V vs.SCE	$h\nu_{CT}$[2] (pyrene·A) 10^3cm^{-1}	color shape	stoichiometry[3] D:A:Solv	IR[4] ν_{CN} cm^{-1} A^0 complex A^-	UV-VIS-NIR[5] 10^3cm^{-1} <20x10^3cm^{-1}	Conductivity[6] σ_{RT} Scm^{-1}	εa meV	Ionicity[7] ob.	es.
1 HCBD	0.72	9.85	dark blue powder	2:2:1(PhCl) (1:1:0.5)	2246 2194 ---	6.3 13.0	$8x10^{-6}$	270	I	I
2 F_4TCNQ	0.60	10.26	green powder	1:1	2227 2197 2193 2213 2178 2178	7.5 14.6	$1.1x10^{-4}$	250	I	I
3 DDQ	0.56	11.76	black powder	1:1	2234 2216 2228 2191	9.8 13.0 19.4	$4.0x10^{-4}$	220	I	I
4 DBDQ	0.54	11.66	black powder	1:1	2230 2212 2214	9.5 12.9 19.2	$2.0x10^{-3}$	190	I	I
5 CF_3TCNQ	0.44	11.60	green powder	2:1	2223 2189 2201 2166 2191 2178	3.3 8.3(sh) 11.5 13.2	$3.3x10^{-1}$	92	P	P
6 F_2TCNQ	0.41	11.59	green powder	3:1	2230 2186 2205 2219 2166 2182	3.8 6.9 12.0 13.0 14.7	$4.8x10^{-1}$	130	P	P
7 DCNNQ	0.38	13.18	black powder	2:1	2234 2199 2200	4.2 12.5	$3.3x10^{-1}$	120	P	P
8 $Q(CN)_2$	0.35	13.61	red powder	7:5	2226 2209 2212	3.5 12.0 18.6	$7.4x10^{-1}$	98	P	P
9 FTCNQ	0.32	12.27	bright green powder	3:1	2221 2180 2200 2178	2.8 7.3 10.8 12.8 14.6	$2.8x10^{-1}$	110	P	P
10 TCNE	0.29	13.55	brown powder	3:1:2(H_2O)	2262 2198 ---- 2228 2163	2.5 11.5	$3.0x10^{-1}$	88	P	P
11 TNAP	0.26	12.76	dark green powder	9:4	2218 2194 2187 2208 2171 2167	2.0 8.8 12.0	$3.0x10^{-1}$	99	P	P
12 DTENF	0.23	14.01	black powder	6:2:1(PhCl) (3:1:0.5)	2233 2182 2190 2159	3.6 8.2 10.7 16.4	$1.9x10^{-2}$	150	P	P
13 TCNQ a	0.22	12.82	dark green powder	1:1	2225 2206 2196 2222 2182	2.8 10.4 17.8	$1.3x10^{-1}$	110	P	P
13 TCNQ b	0.22	12.82	dark green powder	2:1:0.5(DCE)	2225 2206 2196 2222 2177 2182 2153	2.7 11.1 12.8	1.8	77	P	P
14 DCNQ	0.21	14.60	dark red powder	2:1	2236 2199 2206 2225	3.5 11.0 18.6	$1.1x10^{-2}$	100	P	P
15 C_{14}TCNQ	0.21	14.01	grayish green powder	7:2:4(PhCl)	2220 2177 ----	3.1 8.6(sh) 11.4 12.9 14.8	2.7	51	P	P
16 C_{10}TCNQ	0.21	13.61	grayish green powder	11:4:1(PhCl)	2222 2154 2185	2.7 11.4 12.9 16.0	$5.8x10^{-1}$	110	P	P

TABLE IV (Continued)

17 Et_2TCNQ	0.15	13.91	bluish black powder	2:1	2213 2191 2184 2155	2.0 11.2 17.0	3.1	80	P	N
18 Me_2TCNQ a	0.15	13.74	dark green powder	3:1:1(PhCl)	2222 2189 2183 2210 2164	2.4 11.4 13.0 16.5	3.3	70	P	N
18 Me_2TCNQ b	0.15	13.74	black plate	1:1	2222 2205 2183 2210 2164	5.4 16.0	$<10^{-8}$	---	N	N
19 TCNNQ	0.07	14.64	dark brown powder	2:1:0.5(PhCl)	2224 2194 2192 2177 2178	2.4 11.7 17.6	8.1	75	P	N
20 $(MeO)_2TCNQ$ a	0.05	14.71	dark green powder	2:1	2219 2195 2198 2175	2.6 11.3 17.7	3.2	82	P	N
20 $(MeO)_2TCNQ$ b	0.05	14.71	dark red plate	1:1	2219 2211 2198 2175	7.5 17.6(sh)	$<10^{-8}$	---	N	N
21 QCl_4	0.05	15.97	green powder	3:2	----------	3.8 10.7 17.2	4.0×10^{-1}	110	P	N
22 QBr_4	0.04	15.82	black powder	3:1	----------	3.3 11.0	5.0×10^{-1}	110	P	N
23 QF_4	0.04	17.04	gray powder	3:2:2(H_2O)	----------	3.9 11.8 17.8	3.0×10^{-1}	120	P	N
24 BTDA-TCNQ	0.03	14.41	purple powder	5:6:2(PhCl)	2230 2221 2192	7.3 11.8 17.5	$<10^{-8}$		N	N
25 DTNF	0.02	15.62	dark brown powder	3:1:1(PhCl)	2230 2187 2203 2176 2186	3.2 6.5 11.3 17.5	2.3	220	P	N
26 $(EtO)_2TCNQ$	0.01	15.13	dark green powder	2:1	2221 2194 2185 2176 2167	2.4 11.8 17.9	2.1	85	P	N
27 QI_4	-0.02	16.13	black powder	5:4	----------	3.4 11.0	2.6×10^{-1}	100	P	N
28 Me_4TCNQ	-0.05	19.31	only donor	----------	2219 ---- ----	----------	----------		--	N
29 $QBr_2(OH)_2$	-0.12[p]	18.76	black powder	1:1	----------	10.7 12.2 17.9	2.0×10^{-2}	170	N	N
30 $QCl_2(OH)_2$	-0.13[p]	18.66	black powder	1:1	----------	10.6 12.2 18.0	4.0×10^{-3}	300	N	N
31 TENF	-0.14	16.54	brown powder	1:1	----------	9.4 14.1 19.1	$<10^{-8}$	---	N	N
32 Cl_2NNQ	-0.20	17.79	only donor	----------	----------	----------	----------		--	N
33 TCAQ	-0.33	20.75	only donor	----------	2222 ---- ----	----------	----------		--	N
34 $Q(OH)_2$	-0.38[p]	----	dark yellow powder	5:1	----------	11.5	8.0×10^{-3}	97	N	N
35 Cl_2NQ	-0.39	19.69	only donor	----------	----------	----------	----------		--	N
36 TNF	-0.43	18.73	black powder	7:5	----------	10.6 13.8	$<10^{-8}$	---	N	N
37 Q	-0.48	21.79	only donor	----------	----------	----------	----------		--	N
38 TNBP	-0.55[p]	22.12[e,h]	light green powder	ca.5:2	----------	15.6	$<10^{-6}$	---	N	N
39 DNBP	-0.98	----	pink powder	ca.2:3	----------	16.1	$<10^{-8}$	---	N	N

1) Average value of the reduction and oxidation peak-potentials for $A \overset{0}{\rightleftharpoons} A^{-1}$, Pt electrode, CH_3CN, 0.1M TBA·BF_4, 20~22°C, 10~20 mV/sec; p: peak potentials. 2) In $CHCl_3$ solution at RT; sh: shoulder. 3) PhCl :chlorobenzene, DCE:1,2-dichloroethane, 4) CN stretching mode in KBr pellet. 5) In KBr pellet. 6) Conductivity at RT (σ_{RT}) and activation energy (ε_a). 7) I:ionic, P:partial, N:neutral, ob.:judged based on IR, UV-VIS-NIR spectra and conductivity data, es.:judged by Equation (2).

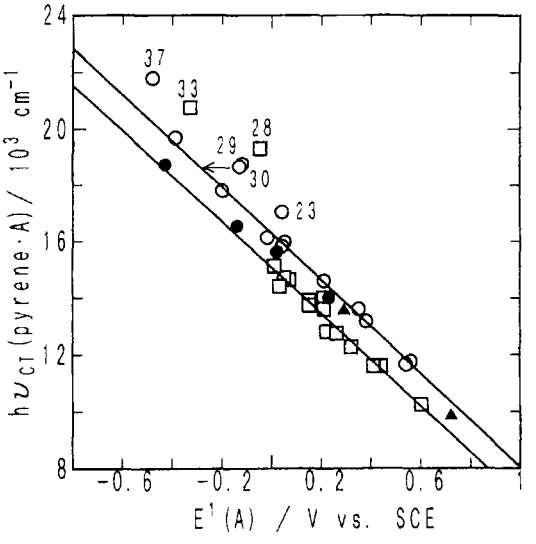

FIGURE 5 A plot of charge transfer band energy ($h\nu_{CT}$(pyrene·A)) *vs.* first redox potential of acceptor molecules (E^1(A)). The numberings correspond to those in Table IV and as for an arrow see text. □:TCNQ system, ○:*p*-quinone system, ▲:percyano system, ●:fluorene system. Lines are least squares fit for TCNQ system (excluding 28, 33) and for p-quinone system (excluding 23, 29, 30, 34, 37).

is lightly affected by solvation energy is said to be a better parameter than E^1(A) to represent the acceptor strength; E_A. The same is true for the $h\nu_{CT}$(D·TNB) and [$h\nu_{CT}$(D·TNB)−$h\nu_{CT}$(pyrene·A)] values against the E^1(D) and ΔE(DA) values to represent I_D and (I_D − E_A) values, respectively. However, it is practically impossible to measure the $h\nu_{CT}$ values for very weak acceptors (or donors) and anion (or cation) molecules. So, we will use the E^1(A) and E^1(D) values in the following discussion with taking into account of the size and shape effect.

Stoichiometry

The color, shape and stoichiometry determined by elemental analysis (C, H, N, S, halogen; the agreement between calculated and observed stoichiometry by elemental analysis is within 0.3%) are presented in Table IV. BEDO-DBTTF is an excellent donor molecule to deliver solid CT complexes even with a weak acceptor, though five very weak acceptors; Me_4TCNQ(28), Cl_2NNQ(32), TCAQ(33), Cl_2NQ(35) and Q(37), which are expected to give neutral CT complexes, did not afford solid complexes even from highly concentrated mixed solution. Good single

crystals of BEDO–DBTTF complexes were difficult to be prepared. It is also noteworthy that the stoichiometry of the complexes between 5 and 27 in Table IV is not simple, namely donor is usually excess in content (3:2, 2:1, 3:1, 4:1) and inclusion of solvent molecules occurs occasionally. These features are reminiscent of the BO complexes,[2] suggesting strong self-aggregation of BEDO–DBTTF molecules in solid complex. It is puzzling that F_4TCNQ and TCNQ gave 1:1 (2, 13a) while F_2TCNQ and FTCNQ gave only 3:1 complexes (6, 9).

IR and UV–VIS–NIR Spectra

In Table IV are summarized the spectral data; the CN stretching frequencies (ν_{CN}) of acceptor molecules in CT complex are compared with those of neutral and anionic species, and the electronic transition energies of solid complex below 20×10^3 cm^{-1}. The CT band energies of neutral ($h\nu_{CT}^{N}$) and ionic ($h\nu_{CT}^{I}$) solid complexes are represented as;[32]

$$h\nu_{CT}^{N} = I_D - E_A - C' + X \quad (3)$$

$$h\nu_{CT}^{I} = -I_D + E_A + (2\alpha-1)C' + X' \quad (4)$$

where α is the Madelung constant, C' is the averaged electrostatic attraction between neighboring donor and acceptor and X and X' are mainly resonance stabilization energies. So the neutral–ionic (N–I) phase boundary condition ($h\nu_{CT}^{N} = h\nu_{CT}^{I}$) gives

$$I_D - E_A = \alpha C' + (X' - X), \quad (5)$$

which is in principle the same as Equation (1). The solid V-shaped line in Figure 6 depicts the Equations (3) and (4), where $\Delta E(DA)$ is used instead of ($I_D - E_A$) and the energy term of the right hand side of Equation (5) is taken as that for the TTF•p-quinone system as proposed by Torrance *et al.*[32b] This V-shaped diagram helps us to predict the ionicity and stacking manner of a CT complex with some care.[32b,33,34]

Neutral Complex – Class I

Ten complexes 18b, 20b, 24, 29, 30, 31, 34, 36, 38 and 39 belong to neutral CT complexes (termed as Class I). This is in good agreement with the estimated ionicity, which is tabulated in the last column of Table IV, based on Equation (2). The IR spectra of them were approximated by the superposition of the neutral component materials.

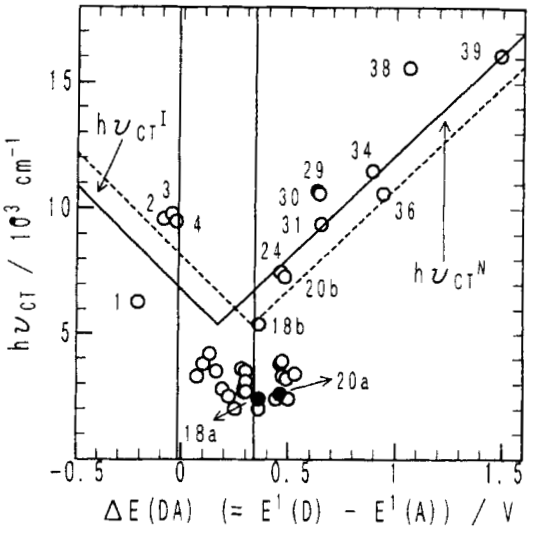

FIGURE 6 A plot of the first transition energy in solid ($h\nu_{CT}$) *vs.* difference of the redox potentials of donor and acceptor molecules $\Delta E(DA)$. The Equations (3) and (4) for TTF•*p*-quinone system are represented by solid V-shaped line. As for dotted V-shaped line, see text. The vertical lines represent Equation (2). The numberings correspond to those listed in Table IV. **18a** and **20a** are depicted by solid circles.

The UV-VIS-NIR spectra of **18b** and **20b** are shown in Figure 7. A CT band is observed at 5.4×10^3 cm^{-1} in **18b**. A band at around 16×10^3 cm^{-1} of **18b** cannot be assigned to those of neutral component molecules. Also it is not ascribable to the intramolecular transition of cation radical (C-band) and anion radical (C'-band, a band originated from the acceptor or anion radical will be discriminated by prime mark), since the complex is neutral. Instead, it is most likely to be the second CT from second HOMO of donor to LUMO of acceptor molecule, since the energy difference of the first and second HOMO of BEDO-DBTTF molecule is *ca.* 12×10^3 cm^{-1}. The complex **20b** also shows the same feature; the band at 7.5×10^3 cm^{-1} to the first CT and that around 18×10^3 cm^{-1} (shoulder) to the second CT transition. The bands at around $23\sim25\times10^3$ cm^{-1} of **18b** and around 22 and 27×10^3 cm^{-1} of **20b** are originated from the intramolecular ones of the acceptor molecules. The donor molecule shows weak absorption above 30×10^3 cm^{-1}.

The first CT bands of Class I complexes locate along the V-shaped

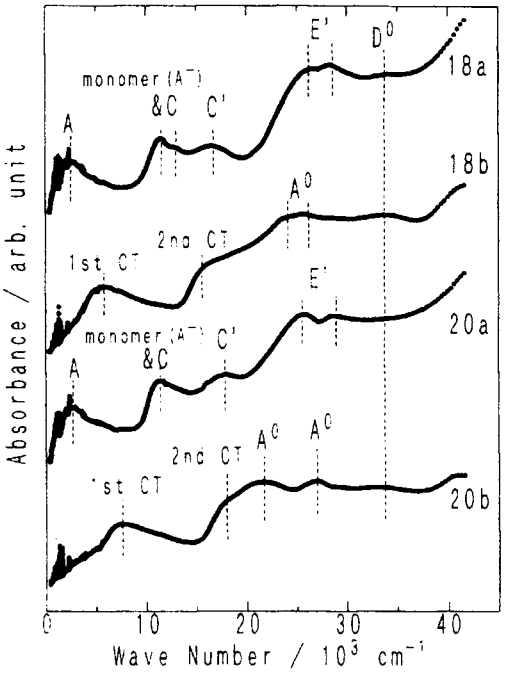

FIGURE 7 UV-VIS-NIR spectra of the Me_2TCNQ complexes (18a, 18b) and $(MeO)_2TCNQ$ complexes (20a, 20b) in KBr disk. For the symbol of each band, see text and Figure 4a.

line in Figure 6 with scatter. Complexes 29, 30 and 38 deviate from the V-shaped line considerably, because their $E^1(A)$ values are peak potentials. A parallel shift of the potentials by 0.14~0.17 V, as mentioned in the section of acceptor strength, for 29 and 30 makes their $h\nu_{CT}$ values close to the line. The same treatment should be taken into account for 34 and 38.

18b locates at considerably low side of the expected V-shaped line for TTF·*p*-quinone system. However, the relation between $h\nu_{CT}$(pyrene ·A) *vs.* $E^1(A)$ in Figure 5 indicates that $E^1(A)$ of TCNQ system deviates from that of *p*-quinone system toward lower side by 0.13~0.16 V. Therefore appropriate V-shaped line of TCNQ system should be obtained by parallel shift of the solid V-shaped line by such difference in $E^1(A)$, provided that the Madelung energy of TTF·*p*-quinone system is not much different from that of TTF·TCNQ system. The dotted V-shaped line in Figure 6 is thus obtained by a shift of +0.16 V in

$\Delta E(DA)$ and **18a** locates on the line.

Ionic Complex - Class III

Four complexes **1**, **2**, **3** and **4** (Class III), all of which are 1:1 stoichiometry, are characterized to be fully ionic based on their IR spectra. For example, it is known that the C=C stretching frequencies at 1600 (b_{2u}) and 1548 (b_{1u}) cm^{-1} of F_4TCNQ^0 show large ionization shift, which are more reliable than the CN stretching frequencies in estimating the γ values.[35] The $K^{\bullet}F_4TCNQ$ shows the bands at 1537 (b_{2u}) and 1503 (b_{1u}) cm^{-1}. However, the bromide salt of BEDO-DBTTF also has broad strong bands at around 1540 cm^{-1}, which overlap with the b_{2u} band. Based on the b_{1u} band of acceptor molecule which appears at 1500 cm^{-1} in the complex **2**, a completely ionic nature of the ground state is identified. The fully ionic character in the complexes of Class III is in good agreement with the estimation based on Equation (2).

However, their first CT bands do not always obey the V-shaped line. The spectrum of the fully ionized DA complex is thought to be composed of the intra- and intermolecular ones of the same kind of component molecules (D^+ or A^-) and/or intermolecular one (back CT; from A^- to D^+) between the different component molecules. In order to identify the back CT defined by Equation (4), the UV-VIS-NIR spectrum of **2** was compared with those of the F_4TCNQ complexes of several TTF derivatives (TTF, ET, BO, DBTTF, TMTTF, HMTTF, TTC_1-TTF, TMTSF, HMTSF), all of which are known to be fully ionic.

There are three kinds of spectrum patterns of them as shown in Figure 8. The first group includes complexes of TMTTF, TMTSF, HMTTF and HMTSF. They exhibit only two bands (B'-band at $6\sim7\times10^3$ and C'-band at $12\sim15\times10^3$ cm^{-1}) below 20×10^3 cm^{-1}, as exemplified by that of the HMTTF complex (Figure 8c) which is known as a Mott insulator.[36] The B' and C'-bands correspond to the inter- and intramolecular transitions of F_4TCNQ anion radical molecules, respectively, as observed in $K^{\bullet}F_4TCNQ$ (Figure 8b). While the bands ascribable to the donor radicals are very weakly observed at $10\sim12\times10^3$ cm^{-1} (B-band) and at $16\sim18\times10^3$ cm^{-1} (C-band), the latter is buried in the very broad C'-band. The transition energies for back CT estimated from the dotted V-shaped line in Figure 6 are indicated by arrows in Figure 8. The

transition energies of the B' and C'-bands do not correspond to the back CT. So it is said that no back CT exists in the F_4TCNQ complexes of the first group. The packing pattern of the F_4TCNQ complexes of HMTTF and HMTSF has been known as segregated one.[36] From the similarity of the UV-VIS-NIR spectra among the complexes of the first group, a similar segregated stacking is expected in the F_4TCNQ complexes of TMTTF and TMTSF.

The second group includes the complexes of TTF, ET (Figure 8d), BO (Figure 8e), BEDO-DBTTF (Figure 8f) and TTC_1-TTF, where there is an additional distinct band at 9~11x10^3 besides the B'- and C'-bands. In the BO complex, however, the band at 9.3x10^3 cm^{-1} appears as a shoulder and strong bands at 12 and 13x10^3 cm^{-1} predominate besides the weak B+B'- (6.7x10^3 cm^{-1}), C'- (15~17x10^3 cm^{-1}), E- (20.0x10^3 cm^{-1}) and strong E'-bands (26x10^3 cm^{-1}). The strong bands at 12 and 13x10^3 cm^{-1}, the latter of which is overlapped with the C-band of BO cation, are due to the isolated F_4TCNQ anion radical which shows bands at 11.7, 13.3 and 24.3x10^3 cm^{-1} in solution (Figure 8a). In the BEDO-DBTTF complex, B'-band is hidden by broad band at 9.6x10^3 cm^{-1} and C- and C'-bands appear at 13~15x10^3 cm^{-1}. While the ET complex shows B+B'-

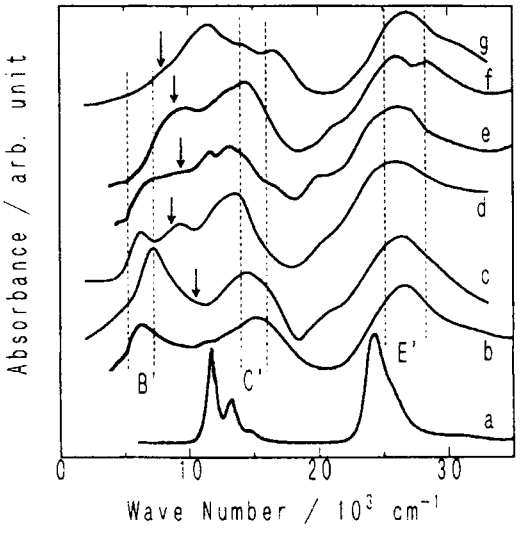

FIGURE 8 UV-VIS-NIR spectrum of F_4TCNQ complex of BEDO-DBTTF (f) is compared with those of F_4TCNQ complexes of HMTTF (c), BEDO-TTF (e), BEDT-TTF (d), DBTTF (g) and K (b) in KBr disk and $K^{\bullet}F_4TCNQ$ in methanol (a). For the symbol of each band, see text. The arrows indicate the predicted positions of the back CT transition.

bands at $6.1x10^3$ cm^{-1}, C' band at $13.6x10^3$ cm^{-1} and the additional band at $9.3x10^3$ cm^{-1}.

It is noteworthy that the band at $9\sim11x10^3$ cm^{-1} appears in the F_4TCNQ complexes when the size of one component molecule exceeds considerably that of the counterpart. Therefore a significant overlap of molecular orbitals of donor and acceptor molecules is conceivable in these complexes, giving rise to a back CT transition. It may be plausible that the newly appeared bands at $9\sim11x10^3$ cm^{-1}, which correspond well to the estimated ones as shown in Figure 8 by arrows, are due to back CT of the F_4TCNQ complexes in this group except TTC_1-TTF·F_4TCNQ, where the observed $h\nu_{CT}$ value ($11.2x10^3$ cm^{-1}) is at fairly high energy side than the estimated one; $h\nu_{CT}^{I}(est)=8.7x10^3$ cm^{-1}.

Meanwhile the transition energy of this band is also in good agreement with that of the B band in the cases of TTF·F_4TCNQ ($10.3x10^3$ *vs.* $12x10^3$ cm^{-1} (intradimer)), BEDO-DBTTF·F_4TCNQ ($9.6x10^3$ *vs.* $10.6x10^3$ cm^{-1}), BO·F_4TCNQ ($9.3x10^3$ *vs.* $9.8x10^3$ cm^{-1} (interdimer)) and with that of the C band in the case of ET complex ($9.3x10^3$ *vs.* $10\sim12x10^3$ cm^{-1}). Also it should be pointed out here that the back CT transition has not yet been detected on a single crystal of ET·F_2TCNQ which is completely ionic and has an alternating stacking.[3c] Based on these facts it is more conceivable that this band corresponds to the lowest intermolecular transition of donor cation molecules (B-band in Figure 4) or the lowest intramolecular transition (C-band in Figure 4). At this moment it is not conclusive whether this band is the back CT, inter- or intramolecular transition of the donor cation molecules, or mixture of them, though the first cause is less plausible, and precise information of the optical properties on single crystals are strongly required for further discussion.

The third group, which includes only DBTTF·F_4TCNQ (Figure 8g), exhibits the bands ascribable to the donor cation radical molecules predominantly. The C'-band is seen as a shoulder ($14.3x10^3$ cm^{-1}) between B- ($11.4x10^3$ cm^{-1}) and C-bands ($16.6x10^3$ cm^{-1}). The B'-band may be buried in the broad B-band. These results are consistent with the non-uniform (dyad) segregated stacking of this complex.[5c] The back CT band is predicted at around $8x10^3$ cm^{-1} for this combination, but there is no trace of such absorption at all.

The DDQ and DBDQ complexes (3, 4) exhibited the B-band (~10.0x10^3 cm^{-1}) and the B'-band (12~13x10^3 cm^{-1}). The latter is the lowest intermolecular transition of the anion radical molecules. The back CT is predicted at far low energy of about 7x10^3 cm^{-1}. Also for the HCBD complex (1), the first (6.3x10^3 cm^{-1}) and second (13.0x10^3 cm^{-1}) bands do not correspond to that expected from Equation (4).

In summary, it is curious enough for the fully ionic complexes studied here, that there are no confidently identified back CT band derived from Equation (4). The observed bands can be assignable to the inter- and intramolecular transitions of the same kind of radical molecules. The stacking manners of them are more likely segregated, however, it is not decisive since alternating stacking complex ET·F_2TCNQ having fully ionic ground state does not exhibit the back CT band but the inter- and intramolecular ones of the same kind of radicals.[3c] From this point of view, caution should be taken for the use of the V-shaped line in the estimation of the stacking manner and ionicity of a CT complex.

Partially Ionic Complex - Class II

All the other 23 complexes (5, 6, 7, 8, 9, 10, 11, 12, 13a, 13b,, 14, 15, 16, 17, 18a, 19, 20a, 21, 22, 23, 25, 26, 27; Class II) in Table IV have the characteristic low-energy band below 5x10^3 cm^{-1} (A-band, for example see curves **18a** and **20a** in Figure 7). The existence of A-band deduces one of the following several electronic and structural states of the complex.

(I) The complex has a uniform segregated 1D column or 2D layer of partially ionized component molecules; either with sufficient transfer interactions (Ia) or insufficient ones (Ib). The former (Ia) gives conventional organic metal as TTF·TCNQ or θ-$(ET)_2I_3$.[37] In the latter case (Ib), complexes are semiconductive owing to the localization of electrons (probably Mott insulator) such as θ-$(ET)_2Cu_2(CN)[N(CN)_2]_2$.[38] The A-band is originated from the intraband process in the former. For the latter the cause of the A-band is still puzzling but maybe related to the intermolecular one among the component molecules having the same fractional charge.

(II) The partially ionized component molecules construct a complex with non-uniform (ex. dyad, triad, etc.) segregated 1D column or 2D layer,

and the lattice distortion splits the HOMO band but does not open a gap at the Fermi level. There are three cases. The first case (IIa) has a partially empty splitted HOMO band, the width of which is larger than the effective U and gives organic metal such as $(TMTTF)_2X$, $(TMTSF)_2X$, β-$(ET)_2I_3$, κ-$(ET)_2I_3$, *etc.*[4] In the second case (IIb), the band width is smaller than the effective U and the system is a Mott insulator where one electron localizes on one site composed of dimerized molecules such as κ-$(ET)_2Cu_2(CN)_3$, β'-$(ET)_2X$ (X=$AuCl_2$, ICl_2) and α'-$(ET)_2X$ (X=$AuBr_2$, $CuCl_2$, IBr_2, $Ag(CN)_2$, $Au(CN)_2$) which have the magnetic susceptibility of more than $7x10^{-4}$ emu/mol at RT. When the band width is comparable to the effective U (IIc), the system is the third case and resides at the boundary between a metal and a Mott insulator. The temperature dependence of electrical resistivity is fuzzy, *viz.* some are metallic and others are semiconductive at higher temperatures, but the magnetic susceptibility is almost temperature independent with $4\sim7x10^{-4}$ emu/mol, such as κ-$(ET)_2X$ (X=$Cu(NCS)_2$, $Cu[N(CN)_2]Br$, $Cu[N(CN)_2]Cl$, $Cu(CN)[N(CN)_2]$).[39] The A-band is the intraband process in (IIa) and the intermolecular process in (IIb), but it is not definite either intraband or intermolecular process in (IIc).
(III) The component molecules are partially ionized, but with a non-uniform segregated stacking due to a Peierls or some lattice distortion which opens a gap at the Fermi level. So they are semiconductive; ex. $TMPD(TCNQ)_2$, $TEA(TCNQ)_2$. The A-band is the interband process.
(IV) The complex is composed of charge separated component molecules with either uniform or non-uniform segregated column or layer; ex. $Cs_2(TCNQ)_3$, $(ET)_8$(Keggin polyoxoanions).[20a] The A-band is the intermolecular process between component molecules with different charges such as $D^0 \rightarrow D^+$ or $A^- \rightarrow A^0$ and the system is semiconductive.
(V) The complex is composed of fully ionized molecules having extremely small effective U with a uniform segregated column or layer. It shows metallic (Va, ex. δ-$(ET)I_3(TCE)_{1/3}$,[31] TTM-TTP$\cdot I_3$[40a], DMTSA$\cdot$X(X=NO_3, BF_4)[40b]) or semiconductive (Vb, ex. BDNT$\cdot PF_6$[19], DMTSF$\cdot$X(X=ClO_4, PF_6)[40b]) behavior. The A-band is the intraband process for the former and the interband one for the latter.

A complex in the case (Ia), (IIa) or (Va) is metallic. Some of them are superconducting. The superconducting complexes having high conductivity in the normal phase owing to the enhanced transfer

interactions by containing selenium, extended π-systems or strong intermolecular atomic contacts exhibit rather low critical temperatures (Tc) of superconductivity as observed in the TMTSF, DMET, BO, DMET-TSF, DTEDT and $M(dmit)_2$ systems.[4] This tendency is also observed among the ET superconductors; namely $(ET)_2I_3$ show high conductivity and normal metallic behavior but the Tc's are lower than the complexes in case (IIc), where Tc's are more than 10K. It is expected that high Tc organic superconductors will be obtained among the poor metals or good semiconductors composed of molecules having rather big U when the crystals satisfy both $U_{eff} \approx$ band width and $t_{\parallel} \approx t_{\perp}$, where $t_{\parallel}$ and $t_{\perp}$ are the transfer integrals within 2D conducting layer. That is one of the motivations for the study of the conductive materials based on BEDO-DBTTF.

The BEDO-DBTTF Class II complexes are not the case (V) since they are composed of partially ionized component molecules as described below. The IR spectra exhibited no coexistence of the neutral and mono-anionic acceptor molecules. As for the donor side the IR spectra of neutral molecule and its radical salt, which might be contaminated with neutral donor since the salt examined is $(BEDO\text{-}DBTTF)_5Br_4(H_2O)_8$, are similar to each other. However, close examination of the spectra revealed that no charge separation occurred in the donor side. Consequently the case (IV) is excluded concerning with both donor and acceptor sides. The semiconductive behavior (next section) of the Class II complexes deny the cases (Ia) and (IIa). As a consequence, the Class II complexes belong to the case (Ib), (IIb), (IIc), or (III).

The IR spectra of TCNQ complexes (13a, 13b) are compared with those of neutral TCNQ and K•TCNQ in Figure 9, in the region of CN stretching. Both 13a and 13b show no trace of band of $TCNQ^0$. The 1:1 complex 13a exhibits only one stretching mode (b_{1u}) at 2206 cm^{-1} indicating both no distortion of segregated column and no charge separation in the complex, though very faint kinks are seen at around 2180 (a_g mode) and 2160 cm^{-1} (b_{2u} mode). So 13a belongs to (Ib) as long as the acceptor column concerns. On the other hand, complex 13b exhibits distinct additional bands besides that at 2206 cm^{-1}; an a_g mode at 2177 and b_{2u} one at 2153 cm^{-1}. In the K salt these bands appear at 2196, 2182 and 2167 cm^{-1}. It should be noted that the band of a_g mode is the strongest among them in 13b. The strong appearance

of a_g mode is indicative of strong lattice distortion (dyad, triad, etc.) of the TCNQ column. Therefore, it is concluded that **13b** has non-uniform column with no charge separation concerning with the TCNQ side (IIb, IIc, III).

The highest frequency band ($b_{1u}\nu_{19}$) of the CN stretching bands of TCNQ molecule is often used to estimate the charge on the TCNQ molecules in its CT complexes.[41] The estimated charge is γ=0.43 for both **13a** and **13b**. This value requires the charge of BEDO-DBTTF as γ=0.43 and 0.22 for **13a** and **13b**, respectively. For other complexes with stronger acceptors than TCNQ in Class II, partial γ values are deduced even with fully-ionized acceptor molecules, since they contain excess donor molecules. The acceptor molecules in the complexes from 5 to 12 are judged as greatly ionic based on their IR spectra. When the acceptor side is completely ionized and forms segregated assemblies, the B'-band should appear in their electronic spectra. The complexes of 5, 6, 9, 10, 11 and 12 are such case and show an absorption peak or shoulder between 5 and 10×10^3 cm^{-1}. Therefore, the degree of CT of BEDO-DBTTF is estimated as 0.3~0.5 for these complexes based on their stoichiometries.

For the complexes with weaker acceptor than TCNQ, it is not easy to estimate the γ value. The IR spectra of **20a** and **20b** are compared

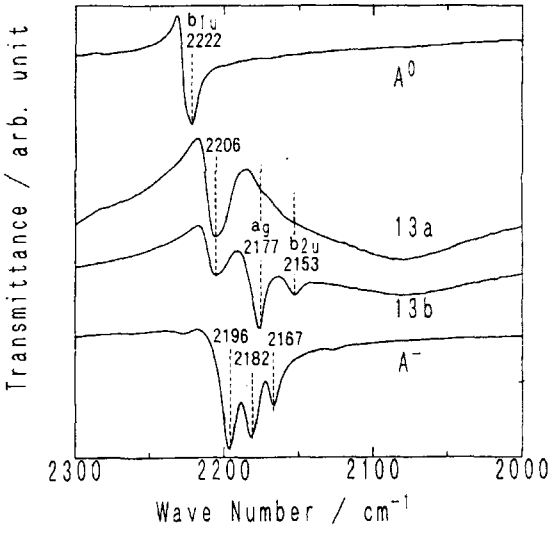

FIGURE 9 Nitrile stretching modes (ν_{CN}) of 1:1 BEDO-DBTTF·TCNQ (**13a**) and 2:1 BEDO-DBTTF·TCNQ (**13b**) are compared with those of $TCNQ^0$ (A^0) and $K^+\cdot TCNQ^-$ (A^-).

with those of neutral and potassium salt of acceptor molecule in the CN stretching range (Figure 10a) and with those of neutral and 5:4 bromide salt of donor molecules in addition to those of acceptor in the range of 1600~400 cm^{-1} (Figure 10b). It is clear that no charge separation or inclusion of A^0 occurs in **20a** and **20b** in the acceptor side. If we use the highest frequency CN band of Li•$(MeO)_2$TCNQ for the estimation of charge on $(MeO)_2$TCNQ molecule, the γ values of $(MeO)_2$TCNQ are 1 and 0.4 for **20a** and **20b**, respectively. If we employed the second highest frequency band the γ values of 0.5 and 0.2 are deduced for **20a** and **20b**, respectively. Since we could not detect the B'-band in the UV-VIS-NIR spectrum of **20a** (Figure 7) the latter estimation(γ=1 for $(MeO)_2$TCNQ) is more acceptable. These γ values are in good harmony with the assignment of the ionicity of the ground state of these complexes based on the UV-VIS-IR spectra in Figures 6 and 7, though these γ values may contain large uncertainty due to the facts that no accurate relation between γ values and CN stretching frequencies has been established for $(MeO)_2$TCNQ and no accurate assignment of the CN mode of $(MeO)_2$TCNQ has been done. These γ values and the stoichiometry of the complexes demand the γ values of the donor side as 0.3 and 0.2 for **20a** and **20b**, respectively. In accordance with this, the IR spectrum of **20b** is approximated as a superposition of those of A^0 and D^0 as shown in Figure 10b. While **20a** shows a superposition of D^0, D^+, A^- and a broad background of electronic transition of the A-band. A similar explanation is applicable to the IR spectra of **18a** and **18b**. Taking account of these results, the electronic spectra of **18a** and **20a** are implied as shown in Figure 7; namely 1) they will not exhibit B-band, 2) B'-band which will appear near $7x10^3$ cm^{-1} is hardly observable since γ values of acceptor molecules are less unity, 3) the bands at around $12x10^3$ cm^{-1} are mainly ascribed to the bands of monomer of anion radical molecules in addition to the C-band, 4) the bands between 25 and $30x10^3$ cm^{-1} are assigned as E'-bands and the band at around $35x10^3$ cm^{-1} is D^0-band.

By assuming a linear ionization shift of the CN stretching of other TCNQs, the γ values of TCNQs and BEDO-DBTTF were estimated for some complexes as following: 0.9 and 0.3 for **16**, 0.6~0.8 and 0.3~0.4 for **17**, 0.8 and 0.3 for **18a**, and 0.8 and 0.4 for **26** in the Class II complexes, while 0.4 and 0.4 for **18b** and 0.2 and 0.3 for **24** in the Class

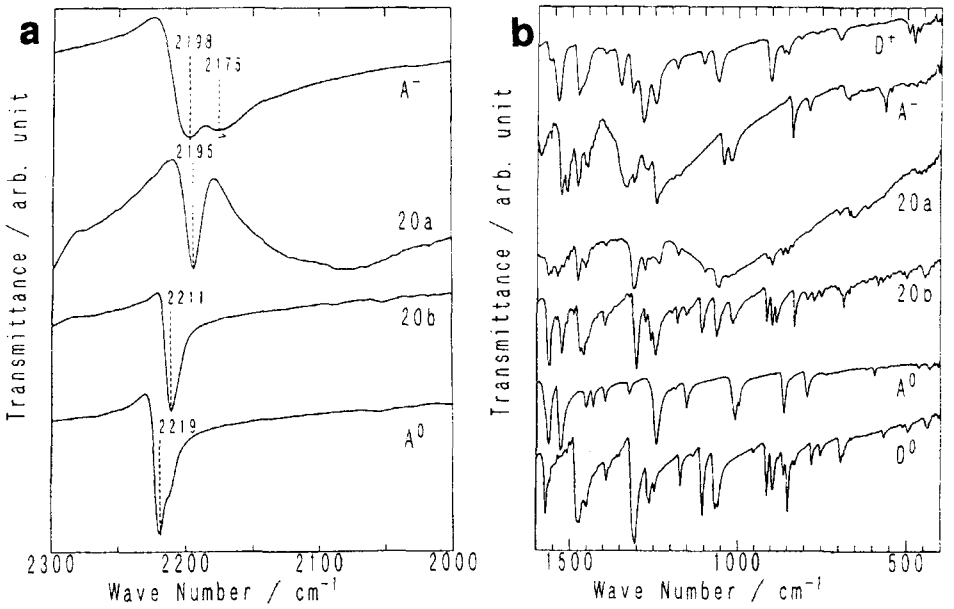

FIGURE 10 IR spectra of 20a and 20b. a) Comparison with those of $(MeO)_2TCNQ$ (A^0) and $Li^+(MeO)_2TCNQ$ (A^-) in the CN stretching range. b) Comparison with those of $(MeO)_2TCNQ$ (A^0), $Li^+(MeO)_2TCNQ$ (A^-), neutral (D^0) and bromide salt (5:4:8(H_2O), D^+) of BEDO–DBTTF between 1600 and 400 cm^{-1}.

I complexes, respectively. Although the accuracy of the estimated γ values may not be excellent for the reasons mentioned above, the lower boundary of the γ value (γ_c) of BEDO–DBTTF in Class II complexes seems to be 0.3.

Unfortunately the spectroscopic data for other acceptor and BEDO–DBTTF molecules and conductivity results so far obtained cannot discriminate the type of the uniformity of the column and the charge. Accordingly further classification requires the detailed knowledge of crystal structures and magnetic susceptibility and will be discussed in the forthcoming paper.

It should be emphasized again that BEDO–DBTTF molecules are able to afford partially ionized CT complexes with a number of acceptor molecules with wide range of acceptor strength, especially even with small degree of CT ($\gamma \geq 0.3$) like BO does. As demonstrated in Figure 6, more than 10 complexes out of 23 ones in Class II locate beyond the vertical line of the right side. This indicates that BEDO–DBTTF can afford partially ionic complexes of segregated type from the

combination with much weaker acceptor molecules (Δ(DA)≤0.53 V) than expected for the conventional TTF·TCNQ type low-dimensional organic metals (Δ(DA)≤0.34 V). This suggests the importance of the ethylenedioxy group in the formation of the self-aggregated donor assemblies in the complexes.

Conductivity

Table IV also summarizes the room temperature conductivity (σ_{RT}) and the activation energy for conduction (ε_a). No single crystals were obtained so far except **18b** and **20b**, so the samples were measured on the compressed pellet. It is seen that the conductivity data have good correlation with the ionicity of the molecule. The conductivity at RT and activation energy for conduction are plotted against ΔE(DA) in Figures 11a and 11b, respectively.

The fully ionic Class III complexes (□) are semiconductive with σ_{RT} less than 10^{-2} Scm^{-1} and ε_a more than 190 meV. Among the neutral Class I complexes (△), **29**, **30** and **34** are fairly conductive with σ_{RT} of 10^{-2}~10^{-3} Scm^{-1} compared with the other Class I complexes of $\sigma_{RT}<10^{-6}$ Scm^{-1}. The ε_a value of **34** is also exceptionally small among the Class I complexes suggesting the hydrogen-bond assisted conduction.

The partially ionic Class II complexes (○) are highly conductive though they are semiconductive. As shown in Figure 11 their room temperature conductivities are mainly more than 10^{-1} Scm^{-1} and activation energies less than 130 meV. *p*-Quinone system has been known to be inferior for producing conductive CT complexes, because of its preference of alternating stack and rather big on-site Coulomb repulsion energy, compared to the TCNQ system. The percyano and fluorene systems have been known to be much more inferior for producing conductive materials. In spite of these facts, BEDO-DBTTF yielded conductive CT complexes. The formation of conducting complexes seems to be only dependent on the redox difference of DA pair, ΔE(DA), though some effect of acceptor molecules may be involved in the rather high ε_a values for fluorene system; **12** and **25**. The σ_{RT} values roughly follow the V-shaped line against the ΔE(DA) values as demonstrated in Figure 11a. The ε_a values also seem to follow V-shaped line some extent. These are reminiscent of that observed in the

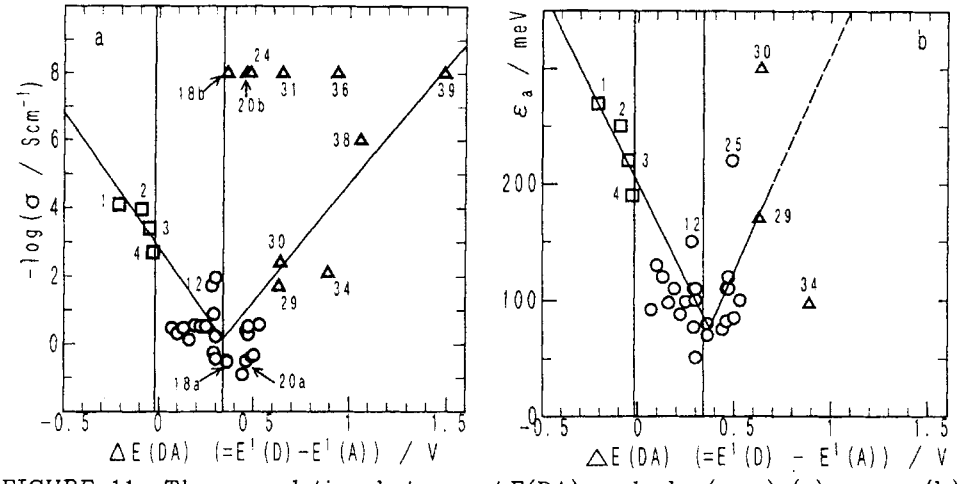

FIGURE 11 The correlation between Δ E(DA) and $-\log(\sigma_{RT})$ (a) or ε_a (b) of the BEDO–DBTTF complexes (△Class I, ○Class II, □ Class III). The vertical lines represent Equation (2). Other lines are guide to eyes. The numberings correspond to those in Table IV.

3,3',5,5'–tetramethylbenzidine(TMB)•TCNQ system,[42] where FTCNQ complex resides at the minimum position of the V–shaped lines and TCNQ complex near the minimum on the neutral branch of the V–shaped lines. The good correlation of the conductivity data with Δ E(DA) values even using a wide variety of acceptor molecules in Figure 11 indicates that BEDO–DBTTF molecules play an essential part for the electron conduction.

It is not decisive experimentally that the semiconductive behavior is due to the barrier between the particles or intrinsic one. However, the BO complexes are metallic even on the compressed pellet samples with σ_{RT} = 10~10^2 Scm^{-1}.[2] So the semiconductive nature is more likely intrinsic one for the BEDO–DBTTF complexes. This is a striking difference between the complexes of BO and BEDO–DBTTF. The good metallic nature of the BO complexes is the consequence of cooperative effects of the strong self–assembling ability and enhanced transfer interactions due to the CH••O and S_{in}••S_{in} contacts and face–to–face π••π interaction. We speculate that the lack of the S_{in}••S_{in} contacts among the BEDO–DBTTF molecules is the reason for semiconductive nature. Nevertheless the self–assembling ability of BEDO–DBTTF molecules due to the CH••O contacts is thought to be stronger than ET and DBTTF, because BEDO–DBTTF provides partially *ionic CT complexes*

with rather weak acceptor molecules.

It has been known that DBTTF prefers alternating stacking with a variety of acceptors, such as F_2TCNQ (with γ=0.6~0.7), FTCNQ, TCNQ (0.47 or 0.25), TCNE, BTDA-TCNQ (~0.25) and TNB and they are insulators.[5] Only with strong acceptors, DBTTF is able to provide conductive complexes, such as Cl_2TCNQ (~0.5), DDQ, DBDQ, and azaTCNQ. However, F_4TCNQ which has a little lower reduction potential than azaTCNQ gave fully ionic dimerized insulator.[5] It is noticeable that DBTTF molecules are able to construct segregated conducting assemblies with a strikingly narrower range of ΔE(DA) values than BEDO-DBTTF, which is a reflection of the lack of both S_{in}··S_{in} and CH··O contacts in the DBTTF complexes.

Based on these conductivity results, it is clearly pointed out again that the ethylenedioxy group has a peculiar ability to enhance the molecules to construct the conductive columns or layers by themselves. The conductivity enhancement of more than eight orders of magnitude is realized by gaining such donor assemblies for **18a** and **20a** compared with **18b** and **20b**.

Complex Isomerization Concerning with Ionicity and Crystal Structure

In the last column of Table IV ionicity of complex judged by the aid of both IR and UV-VIS-NIR spectra and conductivity is presented together with the estimated one from the redox property.

Even though the complexes from 17 to 27 in Table IV are predicted as neutral based on Equation (2), they are in fact partially ionic, and they exhibit low energy CT bands (A-band) located far below the V-shaped line in Figure 6. This is the consequence of easy accessibility of the self-aggregated donor assemblies due to the presence of ethylenedioxy group as mentioned above. Usually self-aggregated assemblies are able to sustain more charge than the alternating ones with the same constituents. For example, black form of TSF·Et_2TCNQ is a metallic complex with segregated stack with $\gamma \geq 0.5$ while red form is an insulator with alternating one with $\gamma < 0.5$.[43] Such monotropic isomers are also known on TMTSF·TCNQ (black form, a segregated metal, γ=0.57~0.63; red form, an alternating insulator, γ=0.21~0.23),[5f,44] ET·TCNQ (triclinic, a segregated metal; monoclinic, an alternating insulator, γ=*ca.* 0~0.2,[3b] TCNQ complexes of 2,7-bis(methylthio)-1,6-

dithiapyrene (triclinic, a segregated metal, γ=0.61~0.71; monoclinic, an alternating insulator, γ=0.31~0.36).[45] The polymorphism having both the different stacking manner and ionicity is one of the complex isomerizations which include the neutral–ionic (N–I) one such as TTF·QCl_4,[46] TTF·QI_4[47] and TMB·TCNQ[48] and the proton– and charge–transfer one such as o–bromoaniline·picric acid[49] and o–dianisidine·TNBP.[50] TTF·QX_4 (X=Cl,I), TMB·TCNQ and o–bromoaniline·picric acid exhibit enanthiotropic complex isomerization.

Complex isomerism has been observed on a DA combination having different kinds of intermolecular interactions when these interactions are approximately equal in strength.[51] In the proton– and charge–transfer system (aromatic amine·polynitrophenol,[49~52] hydroquinone·quinone,[53] biimidazole·TCNQ,[54] *etc.*), progressive weakening of the acid–base (Brönsted type) interaction and strengthening of the CT interaction should produce binary compounds which range in type from "proton–transferred compound" at one end of the series to "CT compound" at the other. In the intermediate situations, same partners form either proton–transferred or CT compounds, depending on ambient conditions.[49,51,52,54] For simple N–I system, which does not include proton–transfer, the essential competing energies are the ionization energy of a DA pair; ($I_D - E_A$), and the Madelung energy of the ionized crystal; (M or $\propto$ C'), regardless whether the system is monotropic or enanthiotropic,[26] and Equation (1) or (5) represents the approximate boundary. In real molecular compounds, the N–I complex isomerization has appeared near the boundary of the neutral and partial CT states; *viz.* upper boundary of Equation (2). In accordance with this, acceptors **18** and **20** gave two kinds of complexes with different ionicity, stacking pattern and physical properties, though they are not strict complex isomers since stoichiometries are different from each other. The Δ(DA) values of the TTF·TCNQ type complexes showing complex isomerization are 0.23, 0.31 and 0.36 V for TMTSF·TCNQ, ET·TCNQ and TSF·Et_2TCNQ, respectively. Compared to these, BEDO–DBTTF affords isomeric complexes with much neutral combination; Δ(DA)=0.46 V for BEDO–DBTTF·$(MeO)_2$TCNQ. That may be the reflection of the extra lattice stabilization energy due to the CH··O interaction in the partial CT form, since the neutral form has a little such interaction in solid state as shown below.

The crystal data of the neutral complexes (18b and 20b) are summarized in Table I. Both have uniform alternating stacking of DADA along the b-axis with the interplanar distances of 3.35 and 3.47 Å for 18b and 20b, respectively. Since both are isostructural to each other, 18b will be described as a representative. The donor and acceptor molecules are almost planar and shows an overlapping mode as depicted in Figure 12a, where the long axis of the acceptor molecule tilts by 13.2° to the long axis of the donor molecule. A unit cell contains two kinds of stackings which are related by screw operation (Figure 12b). The molecular planes of donor and acceptor molecules tilt to the stacking b-axis by 70.4° and 71.4°, respectively. The donor (and acceptor) molecules form side-by-side array along the c-axis with no

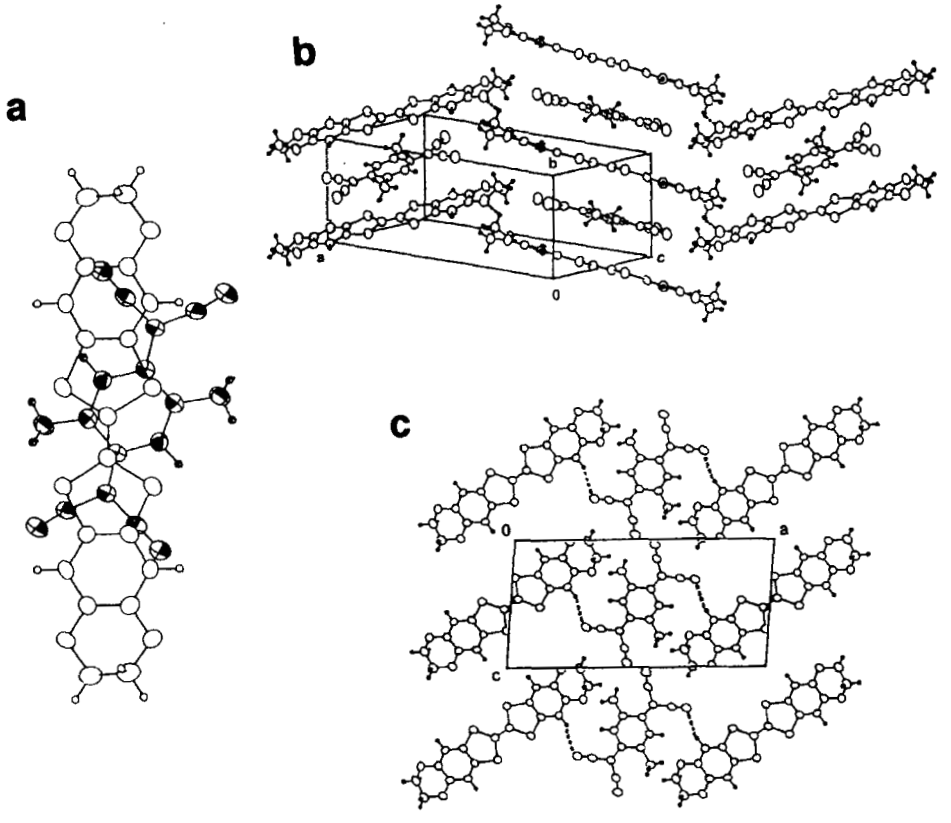

FIGURE 12 Molecular and crystal structures of 1:1 BEDO–DBTTF·Me_2TCNQ (18b). a) Overlapping pattern of donor and acceptor, b) stacking manner in a unit cell, and c) stacking manner in the ac-plane. Short atomic contacts are shown by dotted lines.

short intermolecular atomic contacts less than the vdW radii (Figure 12c). While along the stacking axis, hydrogen-bond like atomic contacts were observed at only two sites; N(12)··H(5) (benzene hydrogen, 2.49 Å *vs.* 2.75 Å) between donor and acceptor molecules and O(1)··H(8B) (ethylene hydrogen, 2.65 Å *vs.* 2.72 Å) among the donor molecules. Other atomic contacts are longer than the vdW sum by more than 0.2 Å. It is worth to place an emphasis on the fact that no short atomic contacts involving sulfur atoms were presented. As a whole, a narrow ribbon of segregated packing manner is only observed along the c-axis and alternating ones along the other two directions. This stacking pattern has much resemblance to that of TTF·QCl_4[55a] rather than perylene·HCBD in which unicomponent sheets of donor or acceptor molecules alternate in one direction and hence is disadvantageous to gain ionicity due to small Madelung gain.[56a] Both TTF·QCl_4 and perylene·HCBD have the $h\nu_{CT}$ values (5.0×10^3 or 5.7×10^3 cm^{-1})[55,56] in the vicinity of the bottom of the V-shaped line in Figure 6. Though the former complex exhibits an N–I transition, the latter does not even at high pressure presumably due to the small Madelung energy and large transfer integral.[56b] From this point it is of interest to study the crystal and electronic structures of BEDO–DBTTF·Me_2TCNQ down to low temperatures. It is also of interest to note that a pronounced switching phenomenon from positive- to negative-resistance in the current *vs.* electric field has been observed on several CT complexes of alternating stack which reside near the N–I boundary.[57] A complex having ionicity closer to the N–I boundary showed the smaller threshold electric field for the switching effect.

CONCLUSION

This work has demonstrated the peculiar ability of BEDO–DBTTF to produce wide variety of conductive CT complexes independent of the size and shape of the acceptor molecules. The presence of the ethylenedioxy groups in BEDO–DBTTF as well as BO provides a pronounced accessibility of conductive CT complexes with smaller degree of CT and from combination with much weaker acceptors than expected with conventional TTF·TCNQ system organic metals. The ethylenedioxy groups of BEDO–DBTTF or BO may assemble donor molecules by CH··O contacts to construct the conductive columns or

layers preferably, and the acceptor molecules serve the functions of charge-compensating and/or space filling. By attaining such assemblies, the conductivity increases more than eight order of magnitude that of the alternating one when each molecule has partial ionicity. Contrary to BO, BEDO-DBTTF afforded not metallic compounds presumably due to the lack of the $S_{in}\cdot\cdot S_{in}$ side-by-side intermolecular atomic contacts in the self-aggregated donor assemblies. That will give us a further guide of a design of new donor molecules.

ACKNOWLEDGEMENT

This work was in part supported by a Grant-in-Aid for Scientific Research from the Ministry of Education, Science, Sports, and Culture, Japan and a Grant for the Proposal-Based Advanced Industrial Technology R&D Program from NEDO, Japan.

DEDICATION

It is our great pleasure to dedicate this paper to Professors Yusei Maruyama and Fumio Ogura on the occasion of their retirement from the Institute for Molecular Science and Hiroshima University, respectively. One of the authors (G.S.) is indebted to Prof. Y.Maruyama for his kind and stimulated discussion and collaboration on the study of organic metals and superconductors. Also G.S. is indebted to Prof. Fumio Ogura for his inspiring ideas on the molecular design of organic metals.

REFERENCES

1) TTF; tetrathiafulvalene, TMTTF, tetramethyl-TTF; HMTTF, hexamethylene-TTF, OMTTF, octamethylene-TTF; DBTTF, dibenzo-TTF; TSF, tetraselenafulvalene; TMTSF, tetramethyl-TSF; HMTSF, hexamethylene-TSF; BEDT-TTF(ET), bisethylenedithio-TTF; EDT-TTF, ethylenedithio-TTF; TTC_1-TTF, tetramethylthio-TTF; TTP, tetrathiapenthalene; TTM-TTP, tetramethylthio-TTP; BDNT, 4,9-bis(benzo-1,3-dithiol-2-ylidene)-4,9-dihydronaphtho[2,3-c][1,2,5]thiadiazole; DMET, dimethyl(ethylenedithio)-diselenadithiafulvalene; DMET-TSF, dimethyl(ethylenedithio)-TSF; DTEDT, 2-(1,3-dithiol)-2-ylidene)-5-(2-ethanediylidene-1,3-dithiole)-1,3,4,6-TTP; dmit, 4,5-dimercapto-1,3-dithiole-2-thione; DMTSA, 2,3-dimethyl-tetraselenoanthracene; TMPD, N,N,N',N'-tetramethyl-p-phenylenediamine; TMB, 3,3',5,5'-tetramethyl-benzidine; TEA, tetraethylammonium; TCNQ, 7,7,8,8-tetracyano-p-quinodimethane; F_4TCNQ, tetrafluoro-TCNQ; Cl_2TCNQ, 2,5-dichloro-TCNQ; CF_3TCNQ, trifluoromethyl-TCNQ; F_2TCNQ, 2,5-difluoro-TCNQ; FTCNQ, fluoro-TCNQ; C_{10}TCNQ, decyl-TCNQ; C_{14}TCNQ, tetradecyl-TCNQ; Me_2TCNQ, 2,5-dimethyl-TCNQ; Et_2TCNQ, 2,5-diethyl-TCNQ;

$(MeO)_2$TCNQ, 2,5-dimethoxy-TCNQ; $(EtO)_2$TCNQ, 2,5-diethoxy-TCNQ; BTDA-TCNQ, bis-1,2,5-thiadiazolo-TCNQ; Me_4TCNQ, tetramethyl-TCNQ; TCNNQ, tetracyanonaphtho-1,4-quinodimethane; TCAQ, tetracyano-9,10-anthra-quinodimethane; TNAP, tetracyanonaphtho-2,6-quinodimethane; aza-TCNQ, 4-dicyanomethylenepyridinium dicyanomethylide; Q, p-benzoquinone; DDQ, 2,3-dichloro-5,6-dicyano-Q; DBDQ, 2,3-dibromo-5,6-dicyano-Q; $Q(CN)_2$, 2,3-dicyano-Q; QF_4, tetrafluoro-Q (p-fluoranil); QCl_4, tetrachloro-Q (p-chloranil); QBr_4, tetrabromo-Q (p-bromanil); QI_4, tetraiodo-Q (p-iodanil); $QCl_2(OH)_2$, 2,5-dichloro-3,6-dihydroxy-Q (chloranilic acid); $QBr_2(OH)_2$, 2,5-dibromo-3,6-dihydroxy-Q (bromanilic acid); $Q(OH)_2$, 2,5-dihydroxy-Q; Cl_2NQ, 2,3-dichloro-1,4-naphthoquinone; Cl_2NNQ, 2,3-dichloro-5-nitro-1,4-naphthoquinone; DCNQ, 2,3-dicyano-1,4-naphthoquinone; DCNNQ, 2,3-dicyano-5-nitro-1,4-naphthoquinone; DTENF, 9-dicyanomethylene-2,4,5,7-tetranitrofluorene; DTNF, 9-dicyano-methylene-2,4,7-trinitrofluorene; TENF, 2,4,5,7-tetranitrofluorene-9-one; TNF, 2,4,7-trinitrofluorene-9-one; TNBP, 3,3',5,5'-tetranitro-biphenyl-4, 4'-diol; DNBP, 4,4'-dinitrobiphenyl; HCBD, hexacyano-1,3-butadiene; TCNE, tetracyanoethylene; and TNB, sym-trinitrobenzene.

2) S.Horiuchi, H.Yamochi, G.Saito, K.Sakaguchi, and M.Kusunoki, J. Am. Chem. Soc., 118, 8604(1996).

3) a) G.Saito, H.Hayashi, T.Enoki, and H.Inokuchi, Mol. Cryst. Liq. Cryst., 120, 341(1985); b) T.Mori and H.Inokuchi, Solid State Commun., 59, 355(1986) and Bull. Chem. Soc. Jpn., 60, 402(1987); c) T.Hasegawa, S.Kagoshima, T.Mochida, A.Izuoka, T.Sugawara, Y.Iwasa, *et al.*, private communication.

4) a) T.Ishiguro and K.Yamaji, Organic Superconductors (Springer Ser. Solid State Sci., 88, Springer, Berlin, 1990); b) J.M.Williams, J.R.Ferraro, R.J.Thorn, K.D.Carlson, U.Geiser, H.H.Wang, A.M.Kini, and H.-H.Whangbo, Organic Superconductors(including Fullerenes): Synthesis, Structure, Properties, and Theory (Prentice Hall, Englewoods Cliffs, NJ, 1992); c) G.Saito, in Metal-Insulator Transition Revisited, edited by P.R.Edwards and C.N.R.Rao (Taylor & Francis, London, UK, 1995), Chap 12, pp231-267.

5) a) H.Kobayashi and J.Nakayama, Bull. Chem. Soc. Jpn., 54, 2408(1981); b) J.J.Mayerle and J.B.Torrance, Bull. Chem. Soc. Jpn., 54, 3170(1981); c) T.J.Emge, W.A.Bryden, F.M.Wiygul, D.O.Cowan, T.J.Kistenmacher, and A.N.Bloch, J. Chem. Phys., 77, 3188(1982); d) G.S.Bajwa, K.D.Berlin, and H.H.Pohl, J. Org. Chem., 41, 145(1976); e) T.J.Kistenmacher, T.J.Emge, F.M.Wiygul, W.A.Bryden, J.S.Chappell, J.P.Stokes, L.Y.Chiang, and D.O.Cowan, Solid State Commun., 39, 415(1981); f) T.J.Emge, F.M.Wiygul, J.S.Chappell, A.N.Bloch, J.P.Ferraris, D.O.Cowan, and T.J.Kistenmacher, Mol. Cryst. Liq. Cryst., 87, 137(1982); g) H.Urayama, G.Saito, T.Inabe, T.Mori, and Y.Maruyama, Synth. Metals, 19, 469(1987); h)T.Suzuki, Y.Yamashita, C.Kabuto, and T.Miyashi, J. C. S. Chem. Commun., 1989,

1102.
6) a) T.Suzuki, H.Yamochi, G.Srdanov, K.Hinkelman, and F.Wudl, J. Am. Chem. Soc., 111, 3108(1989); b) G.Steimecke, H.-J.Sieler, R.Kirmse, and E.Hoyer, Phosphorus and Sulfur, 7, 49(1979); c) K.Hartke, T.Kissel, J.Quante, and R.Matusch, Chem. Ber., 113, 1898(1980); d) G.Saito, H.Hayashi, T.Enoki, and H.Inokuchi, Mol. Cryst. Liq. Cryst., 120, 341(1985); e) J.Nakayama, Synthesis, 1975, 38.
7) refs. 12 and 17 in ref. 2.
8) a) H.Suzuki, K.Nakamura, and R.Goto, Bull. Chem. Soc. Jpn., 39, 128(1966); b) M.Uno, K.Seto, M.Masuda, W.Ueda, and S.Takahashi, Tetrahedron Lett., 26, 1553(1985); c) A,Kini, M.Mays, and D.O.Cowan, J. C. S. Chem. Commun., 1985, 286; d) Y.Nishizawa, T.Suzuki, Y.Yamashita, T.Miyashi, and T.Mukai, Nippon Kagaku Kaishi, 1985, 904; e) B.Helferich, Chem. Ber., 54, 155(1921); f) C.L.Jackson and E.K.Bolton, J. Am. Chem. Soc., 36, 301(1914); g) K.Wallenfels, G.Backman, D.Hofmann, and R.Kern, Tetrahedron, 21, 2239(1965).
9) a) H.W.Underwood,Jr., O.L.Baril, and G.C.Toone, J. Am. Chem. Soc., 52, 4087(1930); b) L.F.Tietze and Th.Eicher, Reaktionen und Synthesen im Organischchemischen Praktikum (George Thieme, Verlag, Stuttgart, New York, 1981).
10) R.Adams, W.Reifschneider, and A.Ferretti, Org. Synth. Coll. Vol. V, 107.
11) A.Ferretti, Org. Synth. Coll. Vol. V, 419.
12) Y.Misaki, H.Fujiwara, T.Yamabe, T.Mori, H.Mori, and S.Tanaka, Chem. Lett., 1994, 1653.
13) C.J.Schramm, R.P.Scaringe, D.R.Stojakovic, B.M.Hoffman, J.A.Ibers, and T.J.Marks, J. Am. Chem. Soc., 102, 6702(1980).
14) The van der Waals radii employed in this paper are as follows; C 1.70, H 1.20, N 1.55, O 1.52, S 1.80 Å. A.Bondi, J. Phys. Chem., 68, 441(1964).
15) N.Sato, G.Saito, and H.Inokuchi, Chem. Phys., 76, 79(1983).
16) The elemental analysis of the bromide salts of DBTTF (DBTTF·Br_2·H_2O;Found(Calcd.) C 34.68(34.87), H 1.97(2.09), O 3.38(3.31), S 26.62(26.59), Br 33.37(33.13)%) and BEDO-DBTTF (BEDO-DBTTF·$Br_{2.1}$·$(H_2O)_{0.8}$;C 35.87(35.87), H 2.26(2.27), O 12.97(12.74), S 21.23 (21.28), Br 27.88(27.84) %) indicates the 1:2 ratio of donor and bromide, but the UV-VIS-NIR spectra of them show the B-band characteristic to monocation state of these donor molecules. Interestingly a 1:1 bromide salt of DBTTF (DBTTF·Br·$(H_2O)_{1.6}$; C 40.62(40.69), H 2.51(2.73), O 6.20(6.19), S 31.13(31.04), Br 19.53(19.33) %) exhibits the A-band at $4x10^3$ cm^{-1} in solid indicating partialy oxidized state of DBTTF. Other bands (B, C, E) appear at the same positions as described in Figure 4d. It is not clear the bromide is Br^{-1} or Br_3^{-1}. In solution both 1:2 and 1:1 salts show very similar spectra. As for the bromide salt of BEDO-

DBTTF, we have obtained 5:4:8(H_2O) salt in addition to the above mentioned 1:2.1:0.8 salt. Both of them show similar spectral feature in solution below $30x10^3$ cm^{-1} but strong band at $31.5x10^3$ cm^{-1} in the 1:2.1 salt was considerably reduced in the 5:4 salt. These bromide salts are under study.

17) A.J.Epstein, S.Etemad, A.F.Garito, and A.J.Heeger, Phys. Rev. B5, 952 (1972).

18) T.Akutagawa and G.Saito, Bull. Chem. Soc. Jpn., 68, 1753(1995).

19) J.Dong, K.Yakushi, and Y.Yamashita, J. Mater. Chem., 5, 1735(1995).

20) a) C.J.Gomez-Garcia, C.Gimenez-Saiz, S.Triki, E.Coronado, P.L. Magueres, L.Ouahab, L.Ducasse, C.Sourisseau, and P.Delhaes, Inorg. Chem., 34, 4139(1995); b) L-K. Chou, M.A.Quijada, M.B.Clevenger, G.F.de Oliveira, K.A.Abboud, D.B.Tanner, and D.R.Talham, Chem. Mater., 7, 530(1995).

21) a) J.B.Torrance, B.A.Scott, B.Welber, F.B.Kaufman, and P.E.Seiden, Phys. Rev. B19, 730(1979); b) T.Sugano, K.Yakushi, and H.Kuroda, Bull. Chem. Soc. Jpn., 51, 1041(1978); c) K.Yakushi, S.Nishimura, T.Sugano, H. Kuroda, and I.Ikemoto, Acta Cryst., B36, 358(1980).

22) G.Saito, K.Yoshida, M.Shibata, H.Yamochi, N.Kojima, M.Kusunoki, and K.Sakaguchi, Synth. Metals, 70, 1205(1995).

23) S.Horiuchi, H.Yamochi, G.Saito, and K.Matsumoto, Mol. Cryst. Liq. Cryst., 284, 357(1996).

24) P.F.Maldague, Phys. Rev. B16, 2437(1977).

25) T.Sugano, H.Hayashi, M.Kinoshita, and K.Nishikida, Phys. Rev. B16, 11387(1989).

26) H.M.McConnell, B.M.Hoffman, and R.M.Metzger, Proc. Natl. Acad. Sci., U.S.A., 53, 46(1965).

27) a) H.Shiba, Phys. Rev. B6, 930(1972); b) Z.G.Soos, S.Kuwajima, and R.H.Harding, J. Chem. Phys., 85, 601(1986).

28) J.B.Torrance and B.D.Silverman, Phys. Rev. B15, 788(1977).

29) a) Y.Matsunaga, Bull. Chem. Soc. Jpn., 42, 2490(1969); b) Y.Matsunaga and G.Saito, Bull. Chem. Soc. Jpn., 44, 958(1971).

30) G.Saito and J.P.Ferraris, Bull. Chem. Soc. Jpn., 53, 2141(1980).

31) a) R.P.Shibaeva, V.F.Kaminskii, and E.B.Yagubskii, Mol. Cryst. Liq. Cryst., 119, 361(1985), b) R.P.Shibaeva, R.M.Lobkovskaya, V.F.Kaminskii, S.V.Lindeman, and E.B.Yagubskii; Sov. Phys. Crystallogr., 31, 546(1986), see also ref. 40.

32) a) R.Foster, Organic Charge Transfer Complexes, (Academic Press, London, 1969); b) J.B.Torrance, J.E.Vaquenz, J.J.Mayerle, and V.Y.Lee, Phys. Rev. Lett., 46, 253(1981). Strictly speaking the intercepts of Equations (3) and (4) should depend upon a specific D•A system.

33) K.Nakasuji, Pure & Appl. Chem., 62, 477(1990).

34) Strictly speaking, the stacking manner is not determined solely from the analysis of the diagram of Figure 6, although such exceptions

are few. Some fully ionic complexes with alternating stacking show the absorptions of CT process among D^+ (or A^-) molecules instead of the back CT absorption (from A^- to D^+) (ex. ET•F_2TCNQ).[3c] Few weak neutral complexes of bezidines and DNBP show a transition from D^0 to A^0, however the complexes have a kind of segregated stacking manner: K.Abe, Y.Matsunaga, and G.Saito, Bull. Chem. Soc. Jpn., 41, 2852(1968).

35) M.Meneghetti and C.Pecile, J. Chem. Phys., 84, 4149(1986).

36) a) J.B.Torrance, Y.Tomkiewicz, R.Bozio, C.Pecile, C.R.Wolfe, and K. Bechgaard, Phys. Rev. B26, 2267(1982); b) J.B.Torrance, J.J.Mayerle, K.Bechgaard, B.D.Silverman, and Y.Tomkiewicz, Phys. Rev. B22, 4940(1980).

37) H.Kobayashi, R.Kato, A.Kobayashi, Y.Nishio, K.Kajita, and W.Sasaki, Chem. Lett., 1986, 789, 833.

38) T.Komatsu, H.Sato, T.Nakamura, N.Matsukawa, H.Yamochi, G.Saito, M.Kusunoki, K.Sakaguchi, and S.Kagoshima, Bull. Chem. Soc. Jpn., 68, 2233(1995).

39) G.Saito, A.Otsuka, and A.A.Zakhidov, Mol. Cryst. Liq. Cryst., 284, 3(1996).

40) a) Y.Misaki, H.Nishikawa, K.Kawakami, S.Koyanagi, T.Yamabe, and M.Shiro, Chem. Lett., 1992, 2321; T.Mori, H.Inokuchi, Y.Misaki, T.Yamabe, H.Mori, and S.Tanaka, Bull. Chem. Soc. Jpn., 67, 661(1994); b) K.Takimiya, A.Ohnishi, Y.Aso, T.Otsubo, F.Ogura, K.Kawabata, K.Tanaka, and M.Mizutani, Bull. Chem. Soc. Jpn., 67, 766(1994). However, anion deficiency in these complexes is possible as well as in δ-$(ET)I_3(TCE)_{1/3}$.[31] The stoichiometries of these complexes have been determined based on only crystallographic analysis without density measurement and/or elemental analysis for only C, H, and N. More precise determination of the stoichiometry is strongly required for these materials to confirm whether the ratio is strictly 1:1 or not. It should be noticed that a few hundred ppm of change of band filling transforms an organic Mott insulator into a metallic and superconducting one due to the drastic decrease of effective U; T.Komatsu, N.Matsukawa, T.Inoue, and G.Saito, J. Phys. Soc. Jpn., 65, 1340(1996). Therefore, neither crystallographic nor elemental analysis is adequate to declare the ratio to be exactly 1:1. It has been reported that the thermoelectric power is close to zero for TTM-TTP•I_3 salt.[40a] It is demanded to study the thermoelectric power which is sensitive to the degree of CT for so called metallic 1:1 complexes more precisely.

41) J.S.Chappell, A.N.Bloch, W.A.Bryden, M.Maxfield, T.O.Poehler, and D.O.Cowan, J. Am. Chem. Soc., 103, 2442(1981).

42)K.Imaeda, T.Enoki, H.Inokuchi, G.Saito, Mol. Cryst. Liq. Cryst., 141, 131(1986).

43) J.R.Andersen, R.A.Craven, J.E.Weidenborner, and E.M.Engler, J. C. S. Chem. Commun., 1977, 526.

44) a) K.Bechgaard, D.O.Cowan, and A.N.Bloch, J. C. S. Chem. Commun., 1974, 937; b) T.J.Kistenmacher, T.J.Emge, A.N.Bloch, and D.O.Cowan, Acta Cryst., B38, 1193(1982).
45) K.Nakasuji, M.Sasaki, T,Kotani, I.Murata, T.Enoki, K.Imaeda, H.Inokuchi, A.Kawamoto, and J.Tanaka, J. Am. Chem. Soc., 109, 6970(1987).
46) a) J.B.Torrance, J.E.Vazquez, J.J.Mayerle, and V.Y.Lee, Phys. Rev. Lett., 46, 253(1981), b) Y.Tokura, S.Koshihara, Y.Iwasa, H.Okamoto, T.Komatsu, T.Koda, N.Iwasa, and G.Saito, Phys. Rev. Lett., 63, 2405(1989).
47) S.Matsuzaki, T.Hiejima and M.Sano, Bull. Chem. Soc. Jpn., 64, 2052(1991).
48) Y.Iwasa, T.Koda, Y.Tokura, A.Kobayashi, N.Iwasawa, and G.Saito, Phys. Rev. B42, 2374(1990).
49) a) E.Hertel, Ann., 451, 179(1926); b) G.Briegleb and H.Delle, Physik. Chem. N. F., 24, 359(1960); c) Y.Matsunaga, E.Osawa, and R.Osawa, Bull. Chem. Soc. Jpn., 48, 37(1975).
50) G.Saito and Y.Matsunaga, Bull. Chem. Soc. Jpn., 46, 1609(1973).
51) a) P.Pfeiffer, Organische Molekulverbindungen, 2 Aufl. (Verlag von F. Enke, Stuttgart, 1927), 341–346; b) F.H.Herbstein, Crystalline π–Molecular Compounds, in Perspectives in Structural Chemistry Vol. IV, edited by J.D.Dunitz and J.A.Ibers (Wiley, New York, 1972); c) G.Saito and Y.Matsunaga, Bull. Chem. Soc. Jpn., 44, 3328(1971).
52) a) G.Saito and T.Inukai, J. Jpn. Assoc. Cryst. Growth, 16, 2(1989).
53) a) T,Mitani, G.Saito, and H.Urayama, Phys. Rev. Lett., 60, 2299(1988); b) K.Nakasuji, K.Sugiura, T.Kitagawa, J.Toyoda, H.Okamoto, T.Mitani, H.Yamamoto, I.Murata, A.Kawamoto, and J.Tanaka, J. Am. Chem. Soc., 113, 1862(1991).
54) T.Akutagawa, G.Saito, M.Kusunoki, and K.Sakaguchi, Bull. Chem. Soc. Jpn., 69, 2487(1996).
55) a) J.J.Mayerle, J.B.Torrance, and J.I.Crowley, Acta Cryst., B35, 2988(1979), b) C.S.Jacobsen and J.B.Torrance, J. Chem. Phys., 78, 112, (1983).
56) a) H.Yamochi, G.Saito, T.Sugano, M.Kinoshita, C.Katayama, and J.Tanaka, Chem. Lett., 1986, 1303; b) T.Ida, K.Yakushi, H.Kuroda, H.Yamochi, and G.Saito, Chem. Phys., 156, 113(1991).
57) Y.Iwasa, T.Koda, S.Koshihara, Y.Tokura, N.Iwasawa, and G.Saito, Phys. Rev. B39, 10441(1989).

APPENDIX

Atomic coordinates and Equivalent Isotropic Thermal Parameters in (BEDO-DBTTF)(Me_2TCNQ)

Atom	x	y	z	B_{eq}
S1	0.01117(7)	0.0944(2)	0.2929(1)	3.24
S2	0.11133(7)	0.0088(2)	0.5237(1)	3.49
O1	0.2085(2)	0.2958(6)	0.0163(3)	3.59
O2	0.3027(2)	0.2365(7)	0.2468(4)	4.05
C1	0.0256(3)	0.0223(8)	0.4625(5)	2.99
C2	0.0975(3)	0.1334(7)	0.2676(5)	2.47
C3	0.1445(3)	0.0975(8)	0.3787(5)	2.80
C4	0.1193(3)	0.1983(8)	0.1468(5)	2.79
C5	0.2123(3)	0.1307(9)	0.3685(5)	3.24
C6	0.1881(3)	0.2305(8)	0.1376(5)	2.77
C7	0.2349(3)	0.2010(8)	0.2491(5)	3.06
C8	0.2815(3)	0.2845(9)	0.0085(6)	3.90
C9	0.3180(3)	0.3523(9)	0.1362(6)	3.96
N11	0.0396(3)	0.7083(9)	0.0389(5)	4.75
N12	0.2053(3)	0.6357(9)	0.3172(5)	4.39
C11	0.0513(3)	0.6665(9)	0.1491(6)	3.49
C12	0.1473(3)	0.6253(8)	0.3058(5)	3.27
C13	0.0747(3)	0.6159(8)	0.2859(5)	2.94
C14	0.0360(3)	0.5598(7)	0.3876(5)	2.64
C15	0.0698(3)	0.5068(7)	0.5155(5)	2.84
C16	0.0390(3)	0.4505(7)	0.6247(5)	2.75
C17	0.0806(4)	0.3977(9)	0.7522(6)	3.70

Atomic coordinates and Equivalent Isotropic Thermal Parameters in (BEDO-DBTTF)[$(MeO)_2$TCNQ]

Atom	x	y	z	B_{eq}
S1	0.3908(1)	0.1326(2)	1.0226(2)	3.41
S2	0.4909(1)	0.0900(2)	0.8028(2)	3.43
O1	0.1988(3)	0.4655(7)	0.7373(5)	3.99
O2	0.2950(3)	0.4295(7)	0.5280(4)	4.15
C1	0.4739(4)	0.0464(8)	0.9637(6)	3.04
C2	0.3593(4)	0.2277(8)	0.8796(6)	2.54
C3	0.4076(4)	0.2100(8)	0.7765(6)	2.69
C4	0.2915(4)	0.3160(9)	0.8652(7)	3.20
C5	0.3855(4)	0.2824(9)	0.6605(6)	2.93
C6	0.2676(4)	0.3859(9)	0.7480(6)	3.05
C7	0.3171(4)	0.3661(9)	0.6460(6)	2.96
C8	0.1817(6)	0.5468(15)	0.6182(8)	5.69
C9	0.2127(6)	0.4643(15)	0.5111(8)	5.87
O11	0.4416(3)	0.4934(6)	1.2370(4)	3.55
N11	0.2942(4)	0.8177(9)	0.8323(6)	4.89
N12	0.4650(4)	0.7235(10)	0.5713(6)	5.18
C11	0.3514(5)	0.7537(9)	0.8182(7)	3.15
C12	0.4510(5)	0.6955(9)	0.6722(7)	3.48
C13	0.4229(4)	0.6727(8)	0.7988(6)	2.49
C14	0.4621(4)	0.5871(8)	0.8966(6)	2.44
C15	0.4285(4)	0.5813(8)	1.0206(6)	2.63
C16	0.4676(4)	0.5008(8)	1.1187(6)	2.49
C17	0.3689(5)	0.5720(12)	1.2635(8)	3.75

Atomic coordinates and Equivalent Isotropic Thermal Parameters in Neutral BEDO-DBTTF

Atom	x	y	z	B_{eq}
S1	0.2696(1)	-0.06432(7)	0.5691(6)	2.81
S2	0.5284(1)	-0.06124(7)	0.9057(7)	3.14
S3	0.4228(1)	0.01886(6)	0.5759(6)	2.63
S4	0.3796(1)	-0.14235(7)	0.8962(7)	3.43
O1	0.0280(3)	-0.1931(2)	0.678(2)	3.78
O2	0.1336(3)	-0.2682(2)	0.993(2)	3.60
O3	0.6497(3)	0.1553(2)	0.796(2)	3.09
O4	0.7526(3)	0.0775(2)	1.096(2)	3.38
C1	0.3678(4)	-0.0785(3)	0.740(2)	2.75
C2	0.4307(4)	-0.0443(3)	0.744(2)	2.59
C3	0.2241(4)	-0.1231(3)	0.698(2)	2.39
C4	0.2749(4)	-0.1600(2)	0.856(2)	2.45
C5	0.5198(4)	0.0395(3)	0.728(2)	2.31
C6	0.5692(4)	0.0024(3)	0.887(2)	2.38
C7	0.1402(4)	-0.1347(3)	0.646(2)	2.78
C8	0.2444(4)	-0.2079(3)	0.953(2)	2.73
C9	0.5477(4)	0.0909(3)	0.700(2)	2.48
C10	0.6467(4)	0.0158(3)	1.011(2)	2.66
C11	0.1107(4)	-0.1830(3)	0.742(2)	2.71
C12	0.1614(4)	-0.2197(3)	0.897(2)	2.66
C13	0.6245(4)	0.1041(3)	0.825(2)	2.56
C14	0.6749(4)	0.0668(3)	0.975(2)	2.50
C15	-0.0037(4)	-0.2384(3)	0.845(3)	4.06
C16	0.0584(5)	-0.2826(3)	0.821(3)	3.74
C17	0.7198(4)	0.1679(3)	1.006(2)	3.37
C18	0.7841(4)	0.1262(3)	0.973(2)	3.68

$B_{eq} = (8\pi^2/3)\Sigma_i U_{ii}$